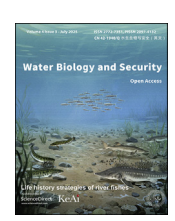
KeA1
CHINESE ROOTS
GLOBAL IMPACT

Contents lists available at ScienceDirect

Water Biology and Security

journal homepage: www.keaipublishing.com/en/journals/water-biology-and-security



Research Article

Neuroprotective Kunitz-like peptides identified from the octopus coral *Galaxea fascicularis* through transcriptomic analysis



Hanbin Chen a,b,c , Hiotong Kam b , Shirley Weng In Siu d , Clarence Tsun Ting Wong e , Jian-Wen Qiu f,g , Alex Kwok-Kuen Cheung c , Gandhi Rádis-Baptista h , Simon Ming-Yuen Lee b,i,j,k,l,m,n,*

- ^a Department of Pharmacology, Joint Laboratory of Guangdong-Hong Kong Universities for Vascular Homeostasis and Diseases, School of Medicine, Southern University of Science and Technology, Shenzhen, China
- b State Key Laboratory of Quality Research in Chinese Medicine and Institute of Chinese Medical Sciences, University of Macau, Macao, China
- ^c Department of Rehabilitation Sciences, The Hong Kong Polytechnic University, Hong Kong, China
- ^d Faculty of Applied Sciences, Macao Polytechnic University, Macao, China
- ^e Department of Applied Biology and Chemical Technology, The Hong Kong Polytechnic University, Hong Kong, China
- f Department of Biology, Hong Kong Baptist University, Hong Kong, China
- ^g Southern Marine Science and Engineering Guangdong Laboratory (Guangzhou), Guangzhou, China
- h Laboratory of Biochemistry and Biotechnology, Institute for Marine Sciences, Federal University of Ceará, Fortaleza, Brazil
- i Department of Food Science and Nutrition, The Hong Kong Polytechnic University, Hung Hom, Hong Kong, China
- ^j PolyU-BGI Joint Research Centre for Genomics and Synthetic Biology in Global Deep Ocean Resource, The Hong Kong Polytechnic University, Hung Hom, Hong Kong, China
- k State Key Laboratory of Chemical Biology and Drug Discovery, The Hong Kong Polytechnic University, Hung Hom, Hong Kong, China
- ¹ Research Centre for Chinese Medicine Innovation, The Hong Kong Polytechnic University, Hung Hom, Hong Kong, China
- m Research Institute for Future Food, The Hong Kong Polytechnic University, Hung Hom, Hong Kong, China
- ⁿ Research Institute for Smart Ageing, The Hong Kong Polytechnic University, Hung Hom, Hong Kong, China

ARTICLE INFO

Keywords: Kunitz-type peptides Neuroprotective effect Potassium ion channel Nrf2 signaling pathway

ABSTRACT

Parkinson's disease (PD) is the second most common neurodegenerative disease. Potassium voltage-gated channels are potential targets for the treatment of PD. The aim of this study is to identify novel potassium ion channel blockers for the treatment of PD through transcriptomic analysis of the coral species Galaxea fascicularis. After annotation by four different databases, four peptides were selected that showed characteristics of potassium ion channel blockers. These four peptides were subjected to multiple sequence alignment and phylogenetic analysis. These four peptides were identified as of Kunitz-type peptides, are known as potassium ion channel blockers. The structures of the peptides were modeled and subjected to molecular dynamics (MD) simulation to verify their stability, which indicated that the peptide GfKuz1 showed the highest potency to block Kv_1 .3 (potassium voltage-gated channel subfamily A member 3) among the reference peptides. The MD simulation of the peptide-protein complexes showed that GfKuz1 interacted with Kv_1 .3, and was more compact and stable than the other potassium ion channel. The blocking effect was confirmed by a potassium ion bioassay. Furthermore, GfKuz1 showed no toxicity to PC-12 cells or zebrafish at concentrations up to 100 μ M. In addition, GfKuz1 increased the PC-12 cell viability that was reduced by 6-hydroxydopamine hydrochloride, and also down-regulated the level of reactive oxygen species and activated the Nrf2 pathway. In summary, GfKuz1 reversed PD symptoms and is a potential peptide drug prototype for PD treatment.

1. Introduction

Parkinson's disease (PD) is one of the most prevalent neurodegenerative diseases, for which the symptoms include tremors, rigid muscles,

bradykinesia, and loss of automatic movements (DeMaagd and Philip, 2015). PD is characterized by the death of dopaminergic neurons in the substantia nigra and the generation of Lewy bodies and alpha-synuclein in intracellular proteins (Hemmati-Dinarvand et al., 2017). Current

https://doi.org/10.1016/j.watbs.2025.100358

Received 19 June 2024; Received in revised form 15 September 2024; Accepted 30 December 2024 Available online 3 January 2025

2772-7351/© 2025 The Authors. Publishing services by Elsevier B.V. on behalf of KeAi Communications Co. Ltd. This is an open access article under the CC BY-NC-ND license (http://creativecommons.org/licenses/by-nc-nd/4.0/).

^{*} Corresponding author. Department of Food Science and Nutrition, The Hong Kong Polytechnic University, Hung Hom, Hong Kong, China. E-mail address: simon.my.lee@polyu.edu.hk (S. Ming-Yuen Lee).

treatment options such as bromocriptine, apomorphine, and ropinirole have undesirable side effects, including insomnia, anxiety, depression, and agitation (Mirza et al., 2015). Recently, more attention has been paid to potassium ion channels as a potential therapeutic target in PD (Chen et al., 2018). Potassium (K⁺) channels located in the central nervous system play an essential regulatory role in resetting resting membrane potential, neuronal excitability, neurotransmitter release, and cellular homeostasis (Lawson and McKay, 2006). The inhibition of potassium ion channels causes excessive excitability of striatum cholinergic interneurons and then reduces Parkinsonism symptoms in a mouse model (Tubert et al., 2016). Therefore, developing pharmacological inhibitors of potassium ion channels may contribute to the treatment of PD and ameliorate its symptoms (Deffains and Bergman, 2015).

Excessive reactive oxygen species (ROS) have been reported to participate in the pathogenesis of some neurodegenerative diseases (Chen et al., 2012). ROS cause prominent PD features like DNA and cellular damage, mitochondrial dysfunction, and neuroinflammation (Cadet and Brannock, 1998; Federico et al., 2012; Peterson and Flood, 2012; Sanders and Timothy Greenamyre, 2013; Fischer and Maier, 2015). In addition, a high level of ROS leads to the death of dopaminergic neurons in PD (Kim et al., 2015). Pervious report has demonstrated that elevated expression levels of antioxidant genes have neuroprotective effects against PD (Williamson et al., 2012). Drugs such as 4-aminopyridine, which inhibit potassium currents, showed an antioxidative effect against ROS and exhibited neuroprotective effects in a PD model (Taherian and Mehran Arab, 2015). Furthermore, 4-aminopyridine treatment could also increase the level of nuclear factor erythroid 2-related factor 2 (Nrf2), linked to an antioxidant pathway (Taherian and Mehran Arab, 2015). Under physiological conditions, Nrf2 binds with its inhibitor Kelch-like ECH associating protein 1 (Keap1) (Itoh et al., 1999). In response to excessive ROS production, Nrf2 is released from Keap1, undergoing cytoplasmic to nuclear translocation and activating heme oxygenase-1(HO-1) production (Taguchi et al., 2011; Ma, 2013). Hence, activation of Nrf2 may play an important role in treating PD (Hemmati-Dinarvand et al., 2019).

Marine biota, including the phylum Cnidaria, have long been recognized as a valuable source of bioactive compounds with potential therapeutic applications. In particular, the octopus coral *Galaxea fascicularis*, a member of the Cnidaria phylum, has gained attention due to its rich repertoire of biologically active polypeptides. According to the Compendium of Materia Medica, members of this phylum have been widely used in traditional Chinese medicine to treat some Parkinsonism symptoms (Ptak, 1990), but the mechanism remains unclear. *G. fascicularis* (class Anthozoa) is a massive coral of the Indo-Pacific oceans. One of the most significant components of their tissues are the biologically active polypeptides that exhibit a high potential for drug discovery due to their high diversity, selectivity, and affinity with target proteins (D'Ambra and Lauritano, 2020; Klompen et al., 2020). Still, few of them have been recognized for their therapeutic potential (Rocha et al., 2011).

The aim of this study is to identify bioactive peptides that have the potential to address PD from the tissues of G. fascicularis through transcriptomic analyses. A phylogenetic tree was constructed to evaluate the relationships between these peptides and other known peptides. We then employed homology modeling and molecular dynamics (MD) simulations to construct their 3D structures and assess their stability. ZDOCK (a protein-protein molecular docking software) and MD simulations were utilized to predict the interactions between the peptides and potassium ion channels. The inhibitory effect of the peptides on potassium ion channels was examined using a potassium ion probe. Following this, the neuroprotective effects of the peptides were evaluated both in vitro and in vivo. Among the biological experiments, one peptide exhibited remarkable neuroprotective activity. Our findings indicate that biologically active polypeptides derived from corals could serve as potential candidates for development into therapeutic agents for treating Parkinson's disease.

2. Materials and methods

2.1. Chemicals and reagents

The rat adrenal pheochromocytoma PC-12 cell line was obtained from American Type Culture Collection (ATCC, Manassas, VA, USA). F-12K medium, horse serum (HS), Gibco fetal bovine serum (FBS), penicillin-streptomycin (PS), and trypsin-EDTA were purchased from Life Technologies (Grand Island, NY, USA). Dimethyl sulfoxide (DMSO), 6hydroxydopamine hydrochloride (6-OHDA), thiazolyl blue tetrazolium bromide (MTT), and phenylmethanesulfonyl fluoride were obtained from Sigma-Aldrich (St. Louis, MO, USA). A bicinchoninic acid protein assay kit and enhanced chemiluminescence were purchased from Thermo Scientific (Rockford, IL, USA). A radioimmunoprecipitation assay lysis buffer, ROS Assay Kit, and Nuclear and Cytoplasmic Protein Extraction Kit were obtained from Beyotime Biotechnology (Jiangsu, China). A phosphatase inhibitor cocktail was purchased from Roche Applied Science (Indianapolis, IN, USA). Ion Potassium Green-2 AM (a potassium ion indicator) was obtained from Abcam (Cambridge, UK). Nrf2, Keap1, HO-1, glyceraldehyde 3-phosphate dehydrogenase (GAPDH), Histone H3, and HPR-conjugated ANTI-RABBIT IgG were purchased from Cell Signaling Technology (Boston, MA, USA).

2.2. Transcriptomic analysis

The transcriptomic data of *G. fascicularis* was downloaded from http://www.comp.hkbu.edu.hk/~db/CoralTBase (Zhang et al., 2019). The annotation was carried out as follows. First, National Center for Biotechnology Information (NCBI) non-redundant protein sequences (NR), UniProtKB/Swiss-Prot, the Kyoto Encyclopedia of Genes and Genomes (KEGG), EuKaryotic Orthologous Groups (KOG), and Pfam databases were utilized for annotation (Mistry et al., 2021); the cut-off was set to 10^{-6} . Gene Ontology (GO) analysis was carried out using Blast2GO software suite v2.5.0 after obtaining the annotation of NR. The GO weight, annotation cut-off, and validated settings were set to "5", "55", and 10^{-6} , respectively. All sequences were assigned to the KEGG, KOG, and GO groups. The transcriptomic data were imported into the ToxProt and Pfam databases to predict venom-related polypeptides with an E-value of 10^{-5} .

2.3. Multiple sequence alignment and phylogenetic analysis

After obtaining the toxin-like peptides, multiple sequence alignment was then performed using MEGA-X software with the MUSCLE algorithm (Felsenstein, 1985; Saitou and Nei, 1987; Kumar et al., 2018). The reliability of the tree was ensured by conducting 2000 bootstrap replicates.

${\it 2.4. \ 3D\ structure\ modeling\ and\ molecular\ dynamics\ simulation\ of\ putative\ peptides}$

The 3D structures of venom-related polypeptides were modeled using the SWISS-MODEL server (Benkert et al., 2010; Bertoni et al., 2017; Bienert et al., 2016; Guex et al., 2009; Waterhouse et al., 2018). After the modeling, the 3D structures were imported into GROMACS 2018 for molecular dynamics (MD) simulation with the CHARMM 36m force field. Briefly, each system was solvated with TIP3P water and then subjected to energy minimization (5 \times 10^5 steps) or a maximum force of 1000.0 kJ/mol/nm. The canonical ensemble (NVT) and isothermal-isobaric ensemble (NPT) equilibration was set to 5 \times 10^5 steps, with a 2 fs timestep at 310 K. The short-range van der Waals cut-off was set to 1.0 nm, Particle Mesh Ewald was used for long-range electrostatics, and MD production was set to 50 ns. Root mean square derivation (RMSD) was employed to evaluate the stability of the structures. PyMOL software (version 1.8; Schrödinger, LLC) was used to visualize 3D structures.

2.5. Molecular docking and molecular dynamics simulation

The atomic positions of the potassium voltage-gated channel subfamily A channels, encompassing $K_V1.1$ (UniProt ID: Q09470), $K_V1.2$ (UniProt ID: P16389), and $K_V1.3$ (UniProt ID: P22001), were modeled through homology in the SWISS-MODEL platform, utilizing the $K_V1.3$ crystallographic framework (PDB ID: 7SSX) as the reference template. GfKuz1 to 4 (four peptides from *G. fascicularis*) were submitted to the ZDOCK server to predict their binding conformations (S. Liu et al., 2021). The top 10 complexes were evaluated by ZDOCK scores. Protein-peptide interaction was analyzed by the protein-ligand interaction profiler (Adasme et al., 2021).

Based on the annotation from the SwissProt database, K_V1.3 is an ion channel protein spanning across the membrane. To investigate the peptide activity on this ion channel, the transmembrane and extracellular parts of K_V1.3 were studied using an MD simulation. The transmembrane domain of the lipid membrane-embedded K_V1.3 simulation system was generated by a membrane builder in CHARMM-GUI (Jo et al., 2007; Jo et al., 2008; Jo et al., 2009; J. Lee et al., 2016). Briefly, the peptide-K_V1.3 complexes were submitted to the server to construct the system and generate the topology. The CHARMM36m force field was chosen for protein and lipid modeling. The TIP3P water was used to solvate the system, and 150 mM K⁺ and Cl-ions were added to neutralize the system and give a physiological concentration of 150 mM. The final system contained 183,496 atoms and 284 1-Palmitoyl-2-oleoyl-sn-glycero-3-PC (POPC) lipids (141 on top and 143 on bottom) and 40,572 water molecules with a box size of $12.01 \times 12.01 \times 13.82$ nm. Then, energy minimization of the system was carried out (5000 steps), along with NVT and NPT equilibration at 310 K (7.5 \times 10⁵ steps with a 1 fs timestep). The van der Waals interaction cutoff was set to 1.2 nm and the MD simulation ran for 100 ns with a 2 fs timestep; a CHARMM 36m force field and GRO-MACS 2018 was used. Analyses were performed using the GROMACS tools, including RMSD and the hydrogen bond number (Baker et al., 2001).

2.6. Peptide synthesis

The coral peptides GfKuz1 and 4 were synthesized by solid-phase chemistry. The purity exceeded 90%, and the peptides were characterized by HPLC and ESI-MS, respectively (Figs. S1–S8). The peptides were solubilized in Milli-Q water to make a 1 mM stock solution and stored at $-20~^{\circ}\text{C}$ until the experiments.

2.7. Cell culture and cell viability

In this study, we employed the rat pheochromocytoma (PC-12) cell line treated with 6-hydroxydopamine (6-OHDA) as a cellular model of PD. This cell-based model has been extensively utilized to investigate the mechanisms underlying neuronal differentiation, neurosecretion, and the biochemical and pathophysiological characteristics associated with PD (Gouda and Cho, 2022).

PC-12 cells were maintained in F-12K medium containing 10% HS, 5% FBS, and 1% PS, and cultured in an incubator at 37 $^{\circ}C$ with 5% CO₂. The PC-12 cells were seeded in a 96-well plate (6000 to 8000 cells per well) for 24 h. To exam the toxicity of these peptides, different concentrations (ranged from 6.25 to 100 μM) of peptides were added to wells. The toxicity of the peptides was determined by the MTT assay after a 24-h incubation.

To assess the neuroprotective effect of peptides, the PC-12 cells were cultured in a 96-well plate (6000 to 8000 cells per well) for 24 h. The indicated concentrations (ranged from 2.5 to 40 μM) of peptides were added to the wells and incubated for another 24 h, and the peptide solution was then removed and 400 μM 6-OHDA was added and incubated for another 24 h. These groups were designated as the treated groups. The control group underwent no intervention, while the vehicle group was administered solely with 400 μM 6-OHDA. The supernatant was

replaced by MTT and cocultured for 4 h. The MTT solution was then removed, and 100 μL DMSO was used to dissolve formazan crystals. The absorbance (wavelengths at 570 and 690 nm) of DMSO was measured using a microplate reader (BioTek, Winooski, VT, USA). The relative viability of treated groups was calculated and compared with the control group.

2.8. Intracellular potassium measurements

PC-12 cells were seeded in a 12-well plate (80,000 to 100,000 cells per well) and incubated for 24 h. Ion Potassium Green-2 AM probe is a cell-permeable dye that can interact with potassium ions and emits green fluorescence in the cytoplasm, and has been widely used to detect potassium ion fluctuations (Ren et al., 2019; Sekar et al., 2018). Drugs that block the potassium ion channel could inhibit the efflux of potassium, leading to the accumulation of potassium in the cytoplasm and prolonging the duration of action potentials (Bachmann et al., 2020). Different concentrations ranging from 2.5 to 20 μM of GfKuz1 (the most active peptide) were added to the wells and cocultured for 1 h. The control group was established with the normal culture medium without any additions. Then, the supernatant was replaced by 0.1% Ion Potassium Green-2 AM and incubated for 30 min at 37 °C in the dark. Cells were washed three times with PBS and stored in polystyrene Fluorescence Activated Cell Sorting (FACS) tubes for data acquisition. The control and drug treatment groups were differentiated using the CytoFLEX Flow Cytometer (Beckman Coulter Inc., Indianapolis, IN, USA) and at least 10, 000 events were further analyzed.

2.9. Intracellular ROS assay

Exposure of PC-12 cells to 6-OHDA causes an increase in intracellular ROS, which directly damage proteins and mitochondrial functions (Qi et al., 2016). Intracellular ROS generation in PC-12 cells was visualized using the probe 2',7'-dichlorofluorescin diacetate (DCFH-DA). Briefly, the cells were exposed to different concentrations of GfKuz1 for 24 h. Then, $400\,\mu\text{M}$ 6-OHDA was added and incubated for another 24 h. These groups were designated as the treated groups. The control group was established with the normal culture medium without any additions, while the vehicle group was administered solely with 400 μ M 6-OHDA. The cells were harvested and washed by PBS three times and exposed to 0.1% of DCFH-DA for 30 min. ROS fluorescence was observed using a DMi8 microscope (Leica, Wetzlar, Germany). The fluorescence intensity was calculated using ImageJ software version 1.53c (NIH, Bethesda, MD, USA) for comparison with the control of the best performing peptide (GfKuz1) for 24 h. The supernatant was replaced with 400 µM 6-OHDA or 0.1% DMSO and cocultured for 12 h. Cells were then washed with PBS three times and lysed for 20 min on ice with a radioimmunoprecipitation assay (1% phenylmethanesulfonyl fluoride and 1% phosphatase inhibitor cocktail). The cytosol protein and nuclear protein were obtained using the Nuclear and Cytoplasmic Protein Extraction Kit. The mixture was centrifuged at 13,000×g for 15 min at 4 °C. The supernatant was collected to determine the protein concentration via bicinchoninic acid assay; all groups were equalized before the experiment. The samples were electrophoresed to 12% SDS-PAGE and the proteins were transferred to polyvinylidene fluoride membranes. The membranes were exposed to 5% non-fat milk for blocking. Immunoblot analysis was undertaken by incubation with nuclear factor erythroid 2-related factor 2 (Nrf2), Kelch-like ECH-associated protein 1 (Keap1), HO-1, and GAPDH (1:1000) overnight. After washing with Tris-buffered saline with 0.1% Tween® 20 detergent (TBST), the membranes were coated with horseradish peroxidase-conjugated goat anti-rabbit antibody (1:2000) for 4 h, followed by three washes with TBST. The enhanced chemiluminescence advanced Western blotting detection kit was used for visualization of different proteins using the ChemiDoc MP imaging system (Bio-Rad, Hercules, CA, USA). The band intensity was evaluated using ImageJ.

2.10. Effect of GfKuz1 on swimming behavior induced by 6-OHDA in zebrafish

Wild-type AB strain Danio rerio (zebrafish) embryos were purchased from the Zebrafish International Resource Center (University of Oregon, USA) and cultured at the Institute of Chinese Medical Sciences, University of Macau, China (Westerfield, 2000). Zebrafish embryos were kept in an embryo medium at 28.5 °C with a pH of 7.4. The embryo medium contained 13.7 mM NaCl, 25 μ M Na2HPO4, 44 μ M KH2PO4, 540 μ M KCl, 300 μ M CaCl2, 100 μ M MgSO4, and 42 μ M NaHCO3. Ethical approval for the animal experiments was granted by the Animal Research Ethics Committee of the University of Macau, China (ethics number: UMARE-021b-2020).

6-OHDA induces degeneration in both dopaminergic and noradrenergic nerve terminals and cell bodies by inhibiting mitochondrial respiratory enzymes, leading to increase oxidative stress and triggering microglial activation. Furthermore, it has been employed to provoke dopaminergic neuronal loss in zebrafish (Cronin and Grealy, 2017).

72 wild-type zebrafish larvae at the 6-day post-fertilization were divided into six groups and each comprising 12 zebrafish. The zebrafish were incubated with different concentrations ranging from 6.25 to $100~\mu\text{M}$ of GfKuz1 for 24 h, while the control group received treatment solely with the embryo medium in 6-well plate. The survival rate of GfKuz1 on zebrafish were recorded.

In order to assess the impact of GfKuz1 on 6-OHDA-induced dopaminergic neuronal loss in zebrafish, 84 wild-type zebrafish larvae at the 3-day post-fertilization were divided into seven groups and each comprising 12 zebrafish. The zebrafish were exposed to specified concentrations of GfKuz1 ranging from 5 to 40 μ M, either with or without

 $250~\mu M$ 6-OHDA for a duration of 4 days, while the control group received treatment solely with the embryo medium and each group of zebrafish were incubated in a 6-well plate. Subsequently, at 7 days post-fertilization, each larva was placed into individual wells within 96-well plates and makes it one larva per well. The behavior of the zebrafish was then observed using a digital video tracking system (Viewpoint, ZebraLab, LifeSciences). The total distances traveled and swimming trajectories were recorded during each individual's 10-min session.

2.11. Statistical analysis

All values are presented as the mean \pm standard deviation (SD). Statistical significance was assessed using one-way ANOVAs followed by a post-hoc Dunnett's test or post-hoc Tukey's test. Post-hoc Dunnett's test was used when comparing multiple treatment groups to a control or vehicle group. The post-hoc Tukey's test was used when comparing all pairs of treatment groups to each other. Graphs were plotted using GraphPad Prism (GraphPad Software Inc., San Diego, CA, USA) and p < 0.05 was considered statistically significant.

3. Results

3.1. Functional annotation of the G. fascicularis transcriptomes

The transcriptomic data of *G. fascicularis* was annotated in the Nr, SwissProt, KEGG, and KOG databases. In total, the databases contained 70,841 unigenes from *G. fascicularis*, and 44,676 (63.07%), 41,648 (58.79%), 8409 (11.87%), and 18,014 (25.43%) of the unigenes were discovered in the databases, respectively. Venn diagrams were employed

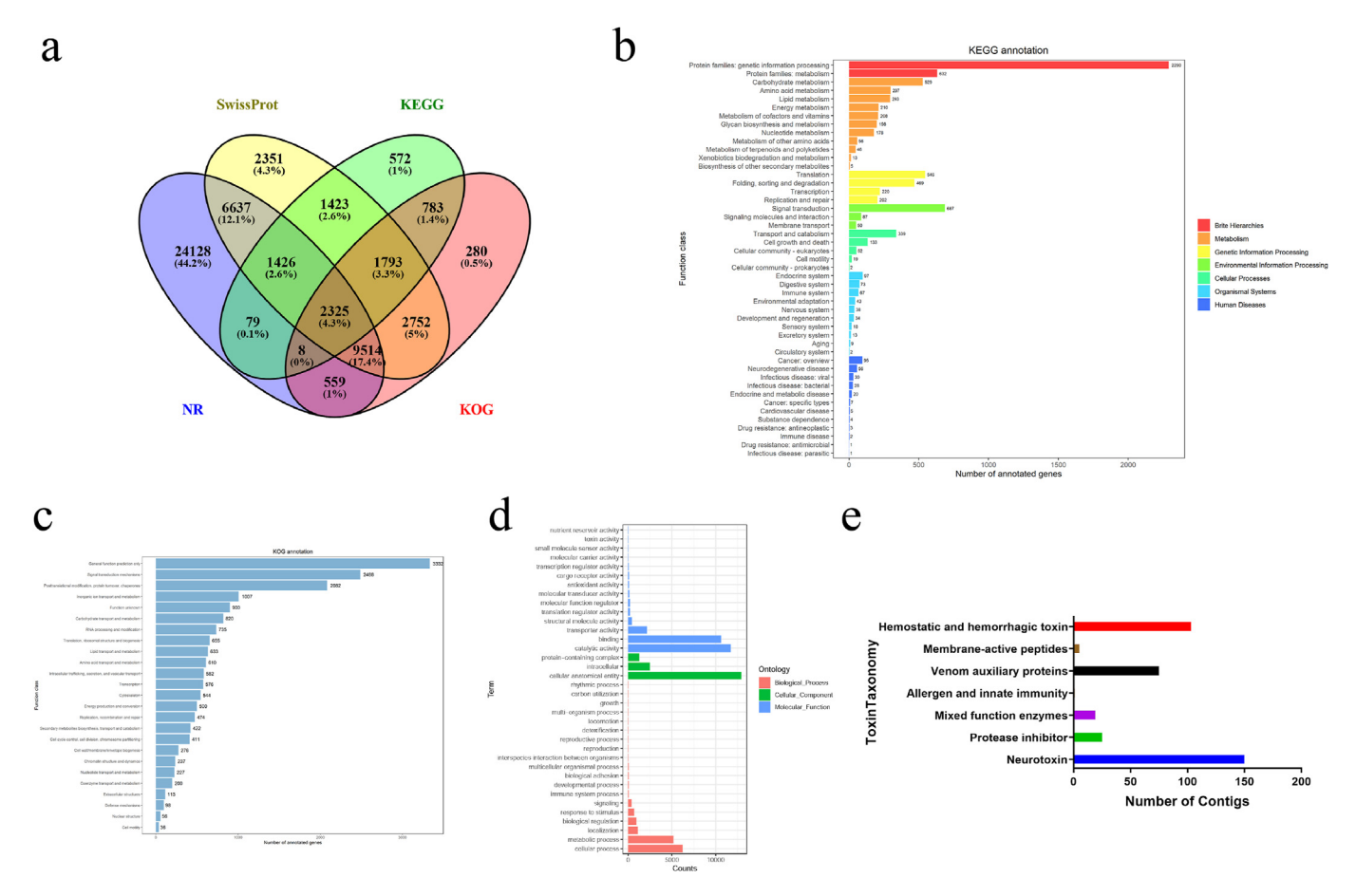


Fig. 1. Functional annotation of *Galaxea fascicularis* assembly. (a) Venn diagram of the unigenes from different databases including SwissProt, KEGG, NR, and KOG. (b) KEGG annotation of the unigenes. (c) KOG annotation of the unigenes. (d) GO enrichment of the unigenes. (e) Taxonomy of putative *G. fascicularis* toxins according to the toxins in the SwissProt database.

for unigene classification based on their characteristics (Fig. 1a). The unigenes were also subjected to the pathway enrichment analysis using the KEGG Automatic Annotation Server. After sequence alignment, they were divided into seven categories (Fig. 1b). The top five most enriched categories of transcripts were genetic information processing (2290, 27.23%), signal transduction (687, 8.17%), metabolism (632, 7.52%), translation (546, 6.49%), and carbohydrate metabolism (529, 6.29%). In total, 18,014 unigenes from G. fascicularis were clustered into 25 species after alignment with the KOG database (Fig. 1c). The most abundant categories in G. fascicularis were general function prediction only (3322 hits), signal transduction mechanisms (2488 hits), and posttranslational modification, protein turnover, and chaperones (2082 hits). After identifying GO-annotated domains by database, the unigenes from G. fascicularis were divided into 36 GO clusters (total of three categories including biological process, cell component, and molecular function) (Fig. 1d). The top five most enriched families of encoded transcript products in G. fascicularis were cellular anatomical entity, catalytic activity, binding, cellular process, and metabolic process (accounting for 20.14%, 18.15%, 17.90%, 12.08%, and 6.08% of the unigenes identified by GO database, respectively).

Descriptions of the putative polypeptide toxins from *G. fascicularis*, based on transcriptomic data, are provided in Table 1. The multialignment and a comparison with the Pfam and Tox-Prot databases revealed 378 toxin-like and venom-related polypeptides from *G. fascicularis*, which were clustered into seven categories. These toxin-like and venom-related polypeptides included membrane-active peptides, auxiliary venom proteins, allergen and innate immunity, mixed-function enzymes, protease inhibitors, hemostatic and hemorrhagic toxins, and neurotoxins.

Kunitz-type peptides are among the most predominant predicted peptides, which include protease inhibitors and ion-channel blockers (D'Ambra and Lauritano, 2020). Some protease inhibitors interfere with potassium ion channels and exert neuroprotective and anti-Parkinsonism effects (Liao et al., 2018, 2019). Based on the annotation from Swiss-Prot and Pfam, four dual-function peptides were selected for further study. These selected peptides were all found to belong structurally to the Kunitz-bovine pancreatic trypsin inhibitor family; therefore, they were named GfKuz1 to 4. The sequence of Kunitz-like peptide toxins identified

Table 1Description of putative polypeptide toxins from the *Galaxea fascicularis* transcriptome.

Toxin group	Toxin family Pfam domain	Num. of contigs	Acc (hmm)	Identity (%
Neurotoxin				
Alpha-latrocrustotoxin	Ankyrin repeats	58	0.73-0.97	30.44–45.3
Alpha-latroinsectotoxin	Ankyrin repeats	23	0.74-0.97	30.51-43.4
Alpha-latrotoxin	Ankyrin repeats	32	0.75-0.97	30.06-41.0
Delta-latroinsectotoxin	Ankyrin repeats	37	0.67–0.98	30.09–45.6
Hemostatic and hemorrhagic toxin				
Coagulation factor V	F5/8 type C	4	0.65-0.95	32.71-39.3
Coagulation factor X	EGF domain	6	0.97-0.98	31.71-53.0
Ryncolin	Collagen triple helix repeat	4	0.42 - 0.87	38.81–54.5
Scoloptoxin SSD14	Gamma-glutamyltranspeptidase	1	0.95	50.00
Veficolin-1	Collagen triple helix repeat	38	0.32-0.95	32.29-60.7
Venom prothrombin activator hopsarin-D	EGF	1	0.97	57.78
Venom prothrombin activator oscutarin-C catalytic subunit	EGF	7	0.7-0.98	32.18–60.0
Venom prothrombin activator oscutarin-C non-catalytic subunit	F5/8 type C	1	0.85	51.06
Venom prothrombin activator porpharin-D	EGF	2	0.94-0.96	44.68–50.0
Venom prothrombin activator pseutarin-C catalytic subunit	Coagulation Factor Xa inhibitory site	3	0.90-0.99	30.21–38.1
Venom prothrombin activator trocarin-D	Trypsin	2	0.98-0.98	43.53–44.2
Venom prothrombin activator vestarin-D1	EGF	24	0.89–1.00	32.50–48.8
Venom prothrombin activator vestarin-D2	EGF	9	0.90-0.98	33.64–47.5
Zinc metalloproteinase-disintegrin jerdonitin	Disintegrin	1	0.92	46.94
Protease inhibitor				
KappaPI-actitoxin-Avd3c	Kunitz/Bovine pancreatic trypsin inhibitor domain	1	0.98	47.37
Kunitz-type serine protease inhibitor	Kunitz/Bovine pancreatic trypsin inhibitor	10	0.94-0.98	38.01-61.6
Turripeptide	Kazal-type serine protease inhibitor	13	0.89-0.98	37.04–60.0
U-actitoxin-Avd3h	Kunitz/Bovine pancreatic trypsin inhibitor	1	0.98	53.45
Mixed function enzymes				
Acetylcholinesterase	Carboxylesterase	2	0.82 – 0.98	37.60-43.4
Augerpeptide hhe9.2	EGF	1	0.95	51.22
L-amino-acid oxidase	NAD(P)-binding Rossmann-like	5	0.79-0.91	32.96-58.3
Putative lysosomal acid lipase/cholesteryl ester hydrolase	Partial alpha/beta-hydrolase lipase region	1	0.96	44.76
SE-cephalotoxin	Thrombospondin type 1 domain	2	0.86-0.98	31.25-35.4
Snake venom metalloproteinase acutolysin-C	Metallo-peptidase family M12B Reprolysin-like	1	0.92	39.56
Venom acid phosphatase Acph-1	Histidine phosphatase	1	0.90	35.35
Venom carboxylesterase-6	alpha/beta hydrolase fold	1	0.76	31.39
Venom peptide isomerase heavy chain	Trypsin	1	0.91	49.02
Venom phosphodiesterase	Somatomedin B domain	4	0.85–0.89	34.18–41.1
Allergen and innate immunity				
Venom allergen 5.01	Cysteine-rich secretory protein	1	0.89	32.32
Venom auxiliary proteins				
Calglandulin	EF hand	65	0.77-0.96	30.00–44.6
Reticulocalbin-2	EF-hand	10	0.73-0.92	30.04–42.6
Membrane-active peptides				
Veswaprin-c	WAP-type (Whey Acidic Protein)	1	0.88	45.10
Waprin	WAP-type (Whey Acidic Protein)	4	0.78 - 0.92	36.74-52.0

from Galaxea fascicularis is shown in Table S1.

3.2. Molecular phylogenetic analysis of candidate peptides

To determine the phylogenetic relationships of selected peptides, we conducted a species-specific search using the BLOSUM62 algorithm in the Blastp suite of the SwissProt database. We included some other related peptides, such as kaliotoxin, margatoxin, HsTx1 (derived from scorpions), and ShK, BgK (derived from sea anemones), which are known to be potent inhibitors of $K_V1.3$. Our analysis revealed that GfKuz1 was closely related to scorpion Kunitz-type peptides, which are predicted to have inhibitory effects on $K_V1.3$. The sequences of GfKuz2 to GfKuz4 were found to originate from a spider (Fig. 2). Therefore, these predicted peptide inhibitors are expected to have a wide range of effects, including anti-cancer, anti-virus, anti-bacterial, anti-inflammation, and voltage-gated potassium ion channel inhibition (Boldrini-França et al., 2020;

Harish and Uppuluri, 2018; Kim et al., 2019; Lin et al., 2004; Soualmia and El Amri, 2018).

Considering the increasing attention given to the pharmacological effects of potassium ion channel blockers for PD treatment, we evaluated the peptides for their potential anti-Parkinsonism effect. GfKuz1 to GfKuz4 were selected for further study (Wulff et al., 2009).

3.3. Homology modeling and molecular dynamics simulation of putative peptides

The 3D structure of four Kunitz-like peptides were built by SWISS-MODEL (Fig. 3). After homology modeling, the stability of peptide structures was investigated. The RMSD of GfKuz1 was 0.30 nm, which indicated that this peptide remained stable during simulation. However, the RMSD values for GfKuz2 and GfKuz3 exhibited significant fluctuations, whereas GfKuz4 demonstrated a relatively steady increase.

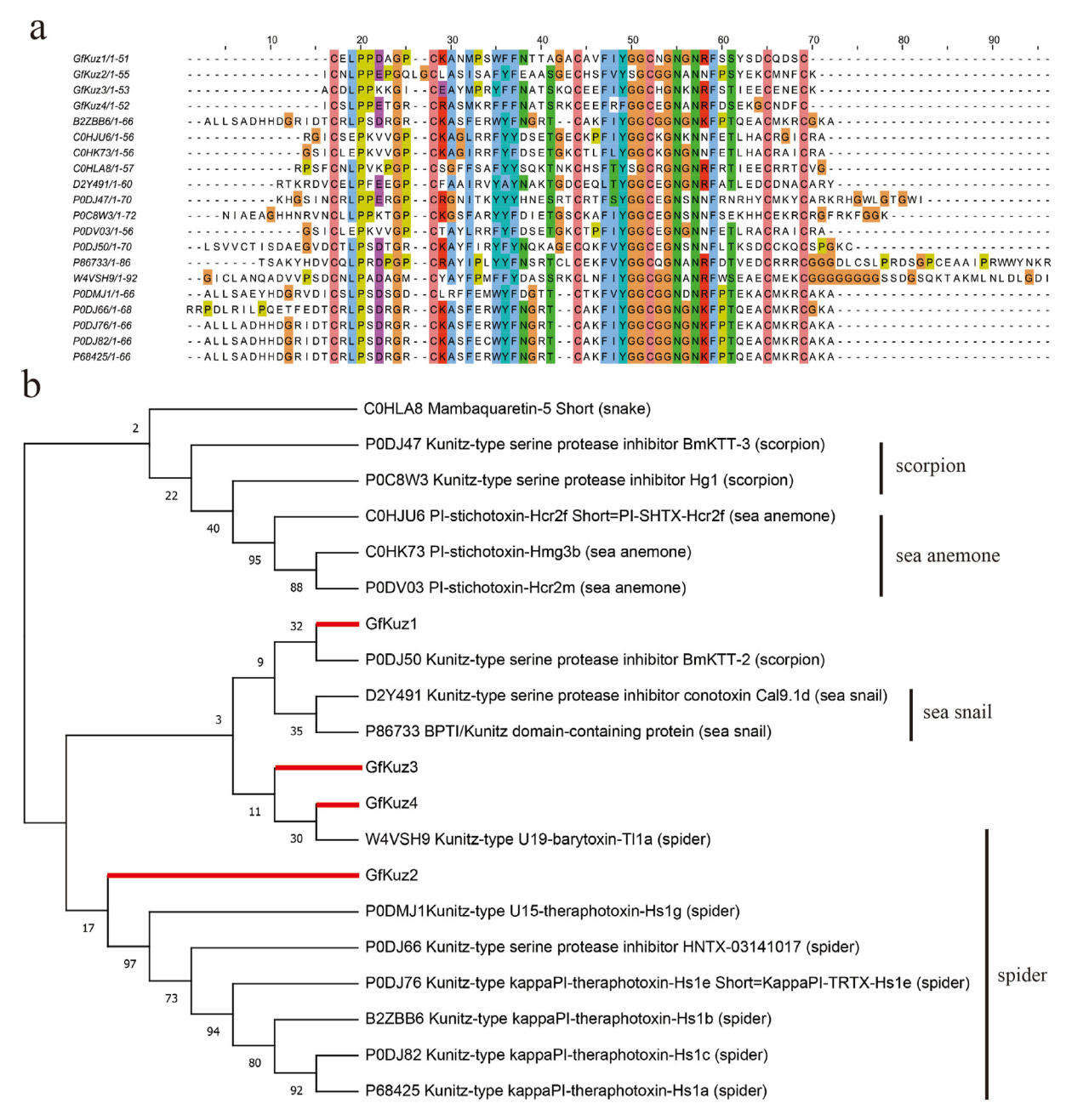


Fig. 2. (a) Multiple sequence alignment and (b) neighbor-joining tree for selected Kunitz-like peptides from G. fascicularis.

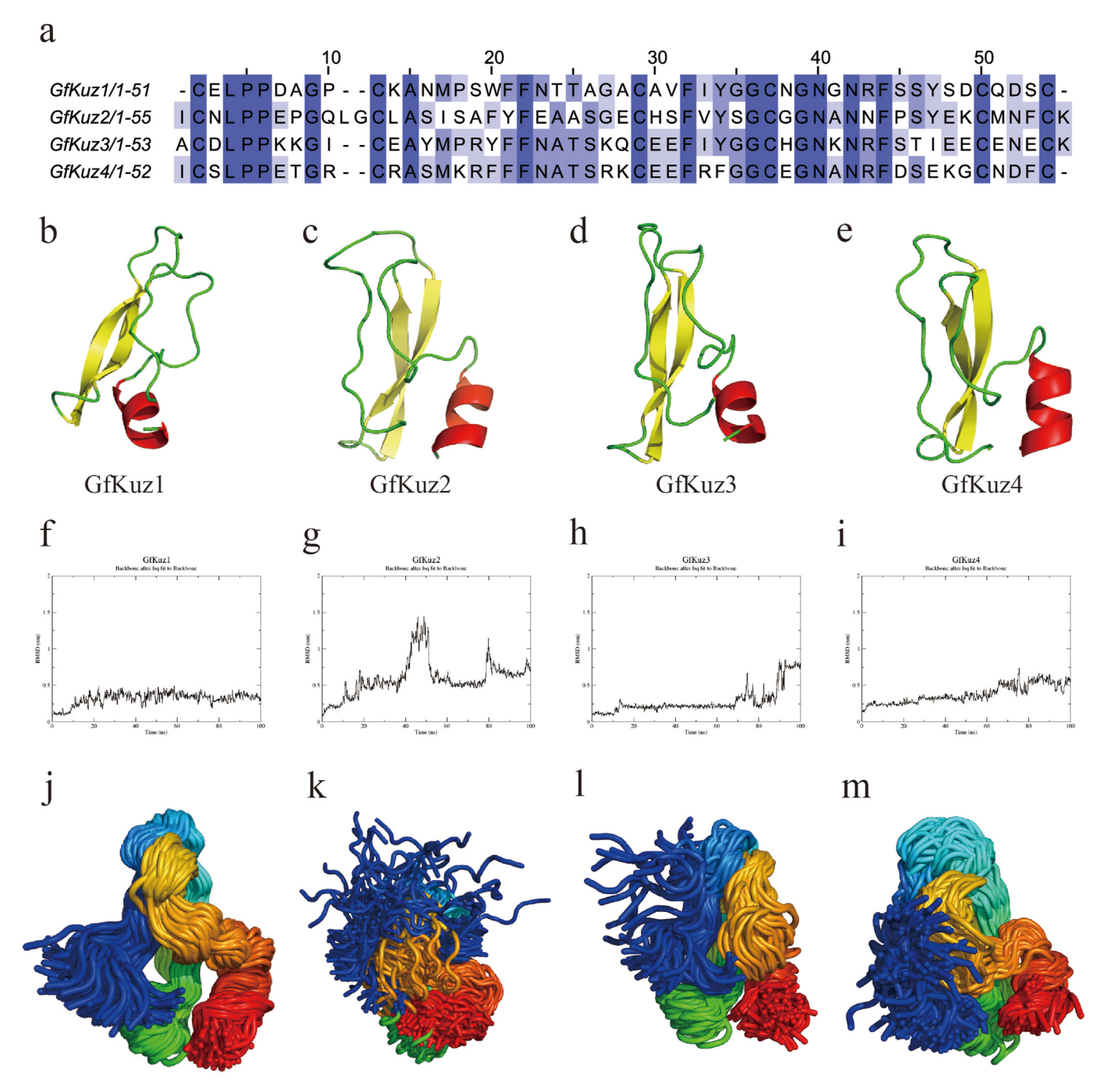


Fig. 3. (a) The amino acid sequences of GfKuz1 to 4. (b–e) The structures of GfKuz1 to 4 were modeled by SWISS-MODEL. (f–i) The backbone RMSD of all atoms of GfKuz1 to 4 after the molecular dynamics simulation via CHARMM36m force field by GROMACS version 2018.6. (j–m) The superimposed structures of GfKuz1 to 4 during molecular dynamics simulation. Different colors were used to represent different regions of peptides.

3.4. Molecular docking and molecular dynamics simulation analysis

From the phylogenetic tree, it is apparent that GfKu1 possesses a potential inhibitory effect on $K_V1.3$, while GfKu2 to GfKu4 each exhibit potential inhibition of potassium ion channels. Subsequently, we selected the three most common potassium ion channels, $K_V1.1$, $K_V1.2$, and $K_V1.3$, and utilized these four distinct peptides for molecular docking with these potassium ion channels. Following the molecular docking conducted by ZDOCK, each group generated 10 complexes. The results indicated that GfKuz1 demonstrated higher scores across various potassium ions, suggesting its potential capability to bind with potassium ions (Table 2). Analysis using the protein-ligand interaction profiler revealed that

GfKuz1 could engage in hydrophobic, hydrogen bonding, and salt bridge interactions with ASP449 in $K_V1.3$, as well as hydrogen bonding and salt bridge interactions with HIS451, both of which were key amino acids that inhibited $K_V1.3$ (Fig. 4) (Liu et al., 2021). This confirmed the

Table 2The docking scores between potassium and peptides.

Scores	K _V 1.1	K _V 1.2	K _V 1.3
GfKuz1	1153.965	1203.33	1254.046
GfKuz2	1192.166	1166.855	1127.996
GfKuz3	1136.989	1114.822	1154.59
GfKuz4	1147.701	1105.263	1045.181

potential inhibitory effect of GfKu1 on $K_V1.3$. The MD simulation was used to analyze the interaction between GfKuz1 and $K_V1.3$.

After the MD simulation study, we obtained data on RMSD and hydrogen bond numbers. Upon binding with GfKuz1, the $\rm K_{V}1.3$ exhibited a more stabilized RMSD value compared to $\rm K_{V}1.3$ alone. The combination of $\rm K_{V}1.3$ and GfKuz1 resulted in an increased number of hydrogen bonds.

3.5. Cell viability and anti-Parkinson effect on PC-12 cells

In vitro studies were employed to determine the potential mechanism

of action of the Kunitz-like peptides from *G. fascicularis*. A MTT assay was utilized to test the toxicity of selective peptides on PC-12 cells (Fig. 5). The concentration of GfKuz1-4 ranged from 6.25 to 100 μM for the PC-12 cell viability assay and from 2.5 to 40 μM for assessing peptide efficacy in cell viability when exposed to 6-OHDA. GfKuz1 and GfKuz2 had no toxicity on PC-12 cells, but 50 and 100 μM of GfKuz3 and GfKuz4 significantly decreased cell viability. After exposure to 6-OHDA, cell viability decreased to about 60% of the control group. GfKuz3 and 4 could not reverse the effect of 6-OHDA. Furthermore, GfKuz1 and GfKuz2 increased cell viability at the indicated concentrations and GfKuz1 exerted a better effect when the concentration was up to 10 μM . This

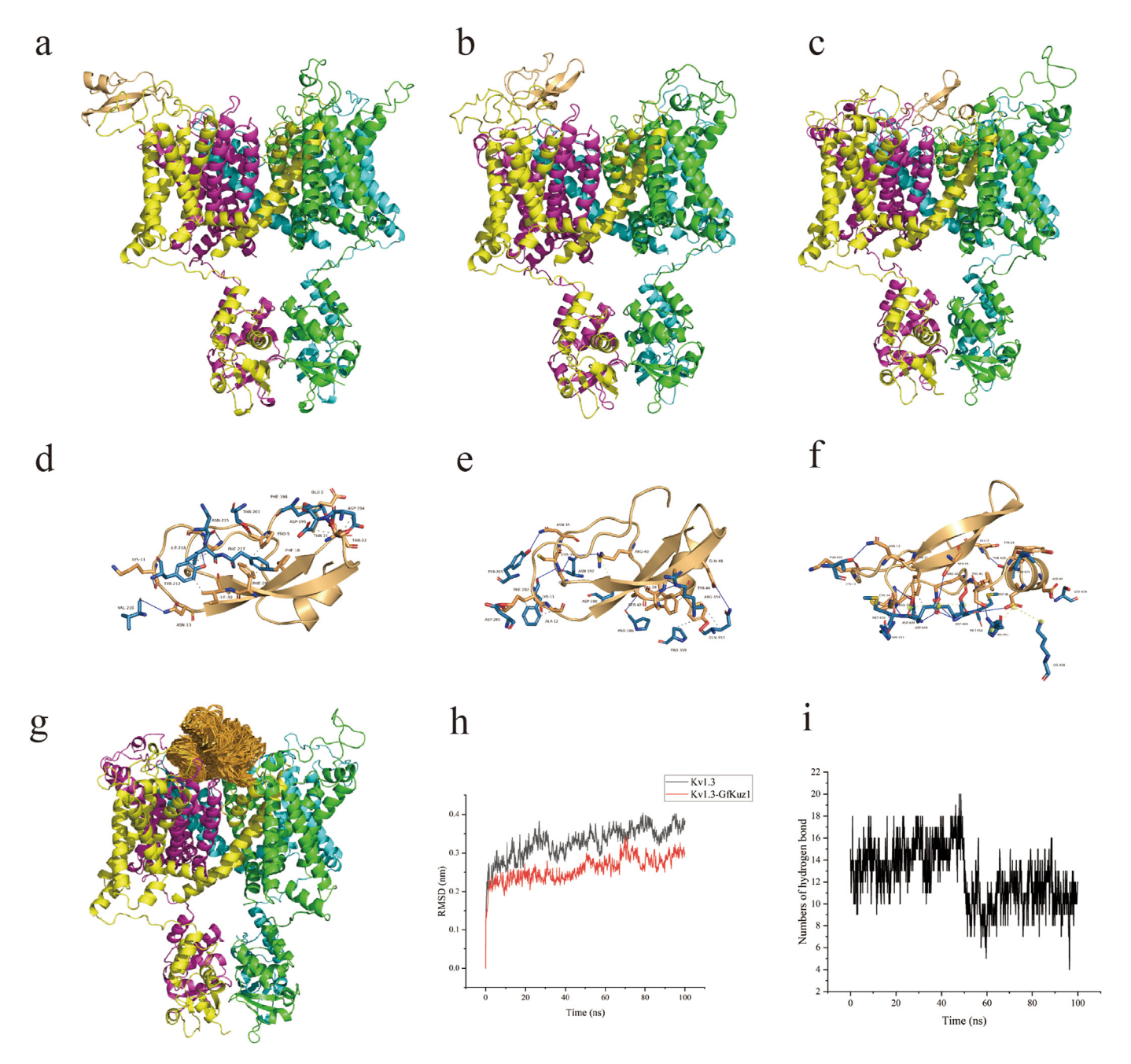


Fig. 4. Molecular docking conformation between potassium ion channels and GfKuz1 from G. fascicularis. Conformation of GfKuz1 docking with $K_V1.1$, $K_V1.2$, and $K_V1.3$; the peptides and proteins were shown as surface mode in PyMOL. (a–c) The peptide is colored light yellow and the different chains of $K_V1.3$ are denoted by different colors. (d–f) The binding modes of GfKuz1 with $K_V1.1$ to $K_V1.3$. The peptides are shown as cartoon mode and colored light yellow. The solid blue line delineates hydrogen bonds, while the dotted lines represent hydrophobic interactions. Additionally, the green dotted lines depict π -cation interactions, and the yellow dotted lines denote salt bridges. Residues are portrayed as sticks. (g) The superimposed structures of GfKuz1 during molecular dynamics simulation when interacting with $K_V1.3$. (h) The RMSD values of $K_V1.3$ during molecular dynamics simulation with or without GfKuz1. (i) The formation of hydrogen bonds between $K_V1.3$ and GfKuz1.

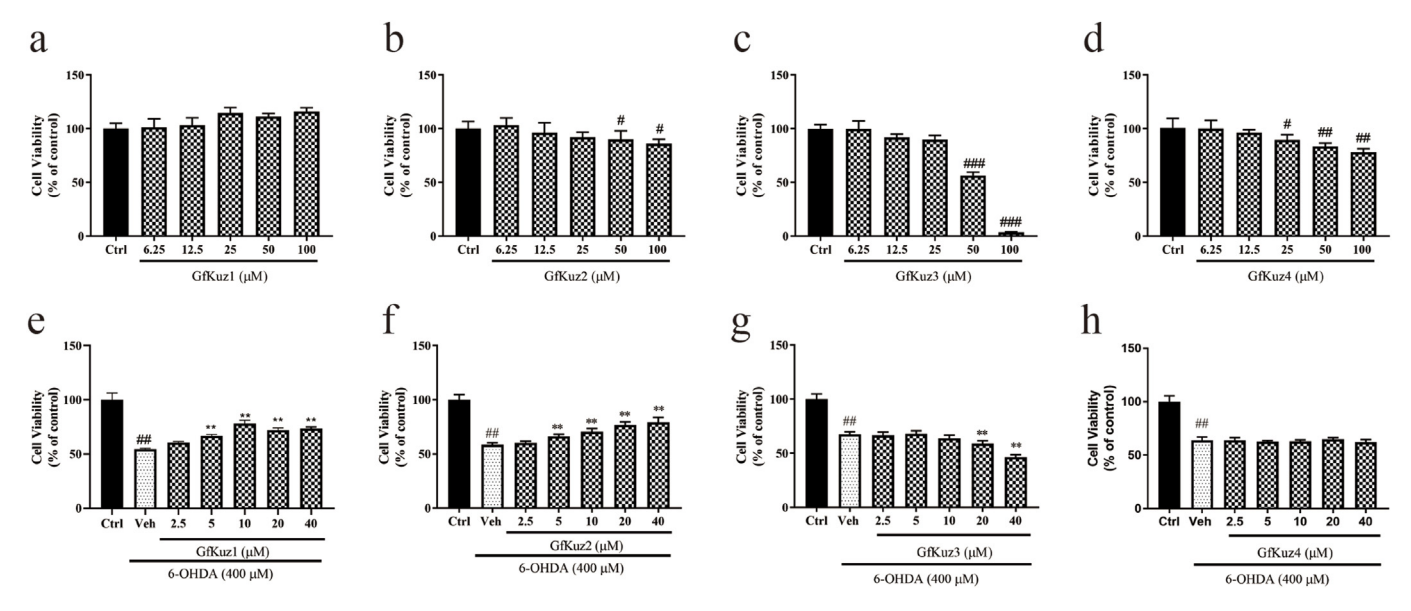


Fig. 5. Effects of coral peptides on the viability of PC-12 cells. (a-d) Effects GfKuz1-4, respectively, on PC-12 cells; (e-h) effects of the corresponding peptides on 6-OHDA-treated PC-12 cells. Data are presented as mean \pm SD (n = 10). ##p < 0.01 vs. control group, **p < 0.01 vs. vehicle group.

implies that GfKuz1 holds the potential for heightened efficacy and potency in the treatment of Parkinson's disease within this specific concentration range. Further investigation or experimentation could help confirm and better understand the differences in efficacy of GfKuz1.

3.6. Determination of the effect of intracellular potassium ion fluorescence on PC-12 cells

Due to the inhibition of potassium ion flow by potassium ion blockers, intracellular potassium ions become elevated. Consequently, peptides capable of suppressing potassium ions were screened based on this

property. Potassium ion probes were used to incubate PC-12 cells stimulated with five different concentrations of GfKuz1 (range: $2.5{\text -}20~\mu\text{M})$ for 24 h, followed by detection using flow cytometry. As shown in Fig. 6a, GfKuz1 significantly increased the potassium fluorescence intensity format at concentrations as low as 5 μM . At the highest concentration of GfKuz1 (20 μM), it elevated the fluorescence intensity to about 30% of the control group. No difference was observed between the 10 and 20 μM GfKuz1 treatments (Fig. 6b). GfKu1 at 10 μM and 20 μM similarly inhibited potassium ion efflux, thereby increasing intracellular potassium ion concentration.

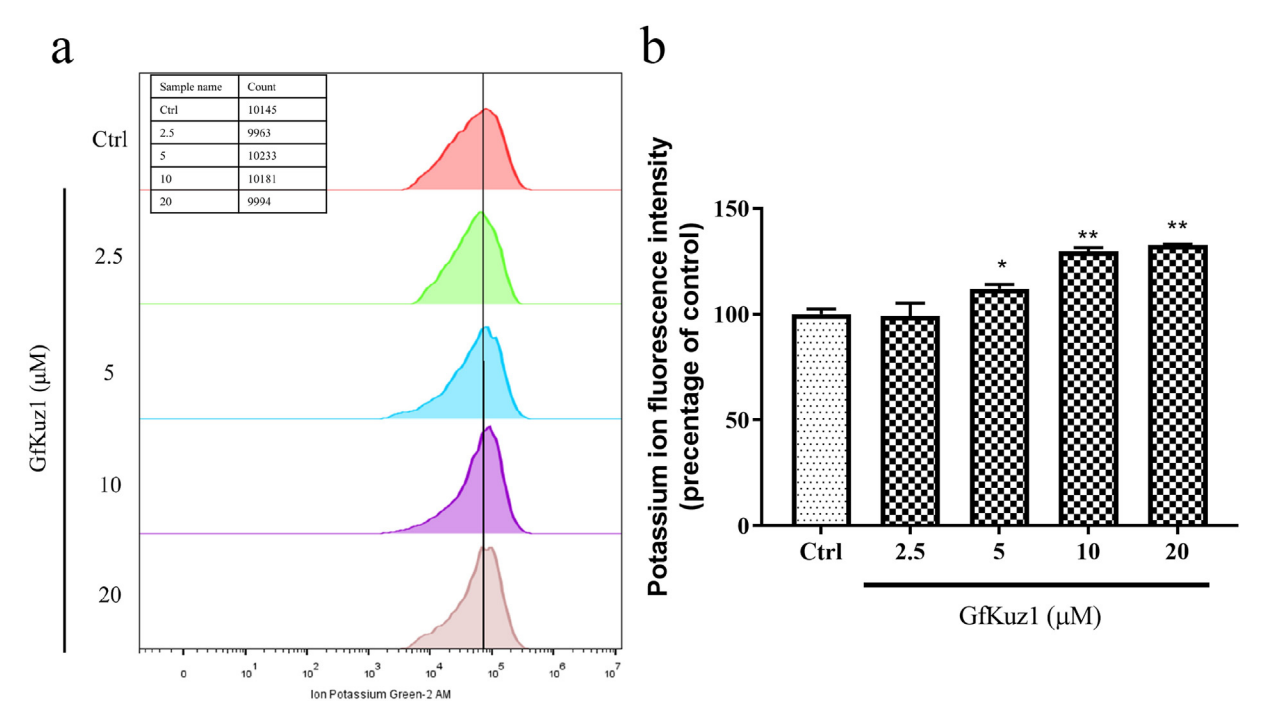


Fig. 6. (a) Quantitative analysis of potassium fluorescence intensity in PC-12 cells by flow cytometry in response to coral peptide (GfKuz1) exposure. (b) Quantitative analysis of the potassium ion fluorescence ratios of different groups compared with the control group. Data is presented as mean \pm SD (n = 3). **p < 0.01 vs. control group, *p < 0.05 vs. control group.

3.7. Determination of ROS activity

The results demonstrated that exposure to 6-OHDA significantly increased the level of ROS by about four-fold in PC-12 cells compared with the control group. After treatment with 2.5 μM GfKuz1, the ROS content dramatically decreased to 168% in cells compared with the 6-OHDA group. The ROS content remained at a normal level after administration of 5 and 10 μM of GfKuz1. Furthermore, treatment with 10 μM of GfKuz1 without 6-OHDA did not affect the level of ROS, as shown in Fig. 7.

3.8. GfKuz1 promoted Nrf2 translocation from cytoplasm to nucleus

As shown in Fig. 8, the expression of Keap1 increased slightly after exposure to 6-OHDA. 5 and 10 μM of GfKuz1 increased the level of Keap1 compared with the vehicle group. 6-OHDA up-regulated the protein expression of HO-1, while 5 and 10 μM of GfKuz1 significantly enhanced the level of HO-1 compared with the vehicle group. As for the Nrf2 protein, exposure to 6-OHDA increased Nrf2 translocation from the cytoplasm to the nucleus. In addition, different concentrations of GfKuz1 promoted translocation compared with the vehicle. Although 2.5 μM of GfKuz1 showed increasing trends of Keap1, HO-1, and Nrf2 translocation, the increases did not reach statistical significance.

3.9. GfKuz1 reversed the abnormal swimming behavior induceed by 6-OHDA

GfKuz1 at concentrations of 6.25–100 μ M was used to assess its toxicity to zebrafish, and GfKuz1 at concentrations of 5–40 μ M was employed to evaluate swimming behavior in zebrafish induced by 6-OHDA. GfKuz1 exhibited no toxicity in zebrafish (Fig. 9a). 6-OHDA decreased the swimming distance of zebrafish. However, different doses ranging from 5 to 40 μ M of GfKu1 increased the swimming distance of zebrafish, demonstrating the significant neuroprotective effect of GfKu1 (Fig. 9b).

4. Discussion

Our study highlighted the potential of Kunitz-type peptides from *G. fascicularis* as novel modulators of potassium ion channels. While the biological functions of Kunitz-type inhibitors are well documented, our

work contributes to utilizing computer modeling and bioinformatic tools to identify the potential inhibitors for potassium ion channels. The identification and structural classification of these peptides into serine protease inhibitors and dual-function inhibitors underscore their diverse functional potential. Notably, the alignment and phylogenetic analysis revealed that these peptides align closely with known potassium channel blockers from various animal venoms, suggesting their potential as new therapeutic agents for conditions like Parkinson's disease. The stability and effectiveness of these peptides in blocking potassium channels, as indicated by MD simulations, point to their promise in developing targeted treatments for PD and other neurodegenerative disorders. This insight into their functional capabilities could lead to significant advancements in pharmacological research and therapeutic applications.

In the present study, four peptides were selected for investigation that was initiated by molecular docking and molecular dynamics (MD) simulations with the three common potassium ion channels K_V1.1, K_V1.2, and K_V1.3. ZDOCK is a fast Fourier transform-based protein docking program widely used to predict the interactions between peptides and proteins (Pierce et al., 2014). ZDOCK generated 10 complexes and the best conformation was selected for binding analysis. Upon integrating the results of ZDOCK, it was discovered that GfKuz1 exhibited a greater propensity than the other peptides to bind with three potassium ion channels. Additionally, within the phylogenetic tree, a potential inhibitory effect of GfKuz1 on Ky1.3 was identified, where GfKuz1 bound at the pore of K_V1.3. The docking results indicated that GfKuz1 interacted more effectively with K_V1.3 (Fig. 3). In addition, GfKuz1 generated hydrophobic interactions, hydrogen bonds, and salt bridges with the key amino acid residues, namely D449 and H451 of K_V1.3 which are involved in the C-type inactivation of K_V1.3 (Liu et al., 2021). The structures were also subjected to MD simulation using GROMACS. The superimposed structure of GfKuz1 remained stable at the pore of K_V1.3. Our results also showed that the K_V1.3-GfKuz1 complex retained a lower RMSD value compared with K_V1.3 and resulted in an abundance of hydrogen bonds. Our data illustrated that GfKuz1 and K_V1.3 reached a dynamic equilibrium and remained stable and strongly bound, which is consistent with the results from the docking experiments. Based on the molecular docking and MD simulation study, GfKuz1 interacted with the active site to block K_V1.3 and then remained more stable, forming a more compact structure compared with other peptides. Therefore, GfKuz1 can be utilized for further research. Meanwhile, further experiments such as patch-clamp are needed to verify whether GfKuz1 serves as a potential

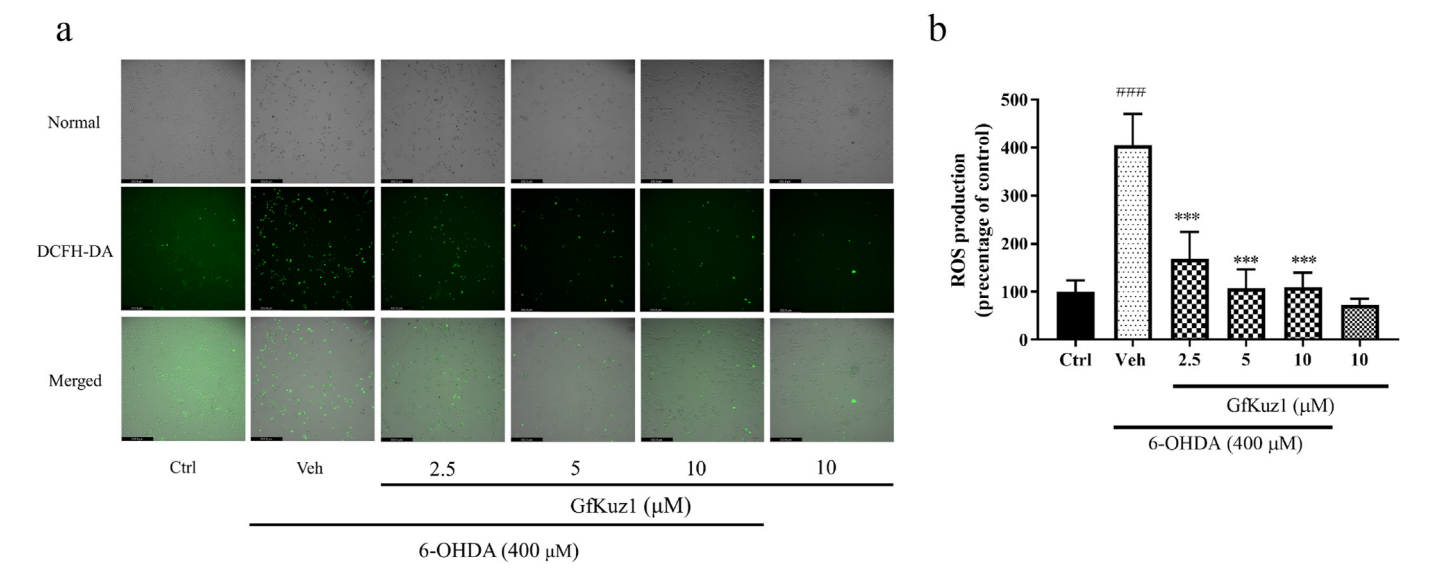


Fig. 7. Reduction of ROS production in PC-12 cells in response to GfKuz1 exposure. (a) ROS production was recorded by DCFH-DA fluorescence, with normal, representative, and merged fluorescence images of PC-12 cells. (b) ROS generation fluorescence ratio in different groups compared with the control group. Data are presented as mean \pm SD (n = 3). ###p < 0.001 vs. control group, ***p < 0.001 vs. vehicle group.

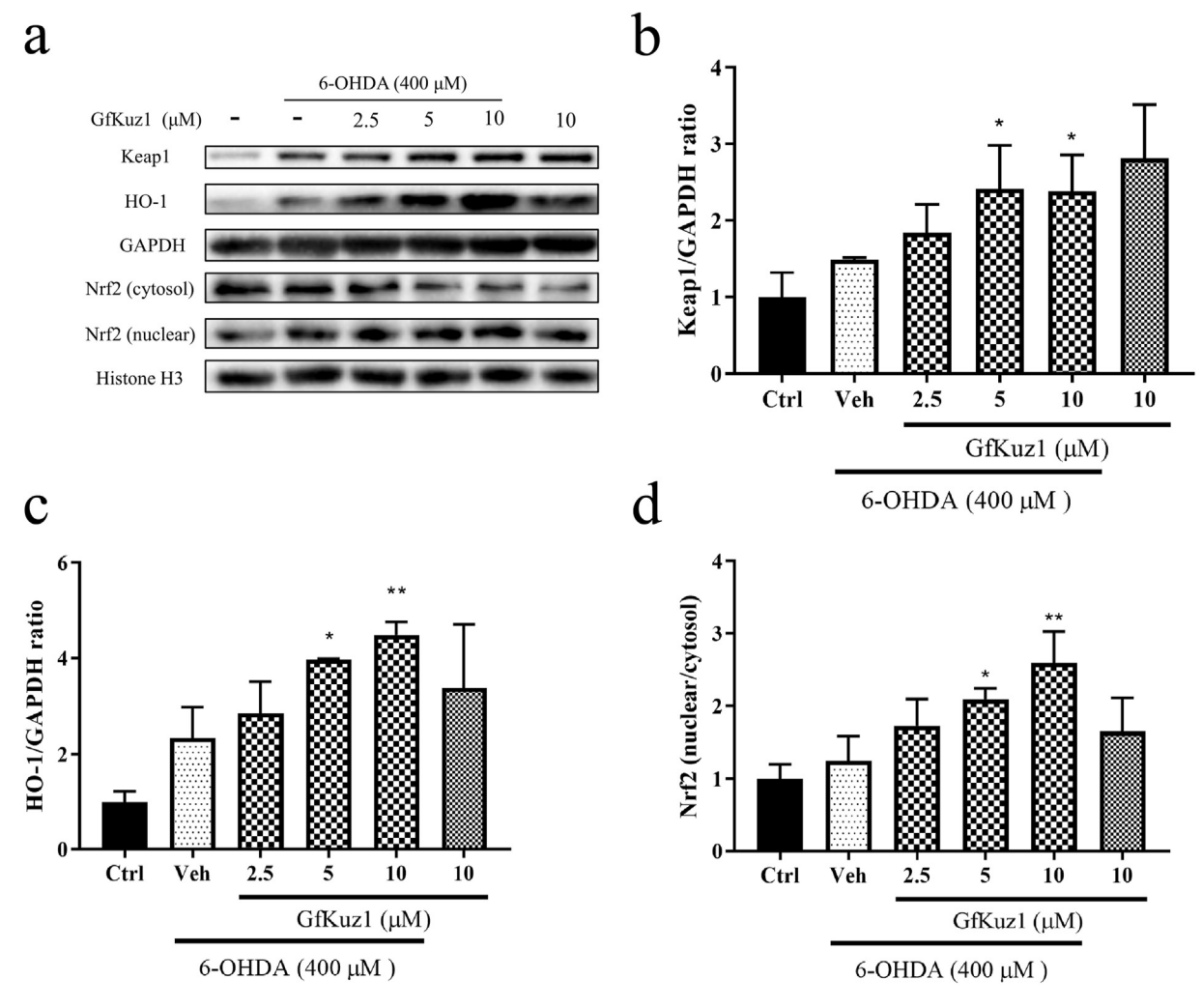


Fig. 8. Effect of GfKuz1 on the Nrf2 nuclear translocation and Nrf2/HO-1 signaling pathway. (a) Western blotting analysis of the protein expression of the Keap1, HO-1, and cytoplasmic and nuclear Nrf2 of PC12 cells exposed to 6-OHDA in the presence or absence of different concentrations of GfKuz1. (b) Quantitative analysis of the density of Keap1. (c) Quantitative analysis of the density of HO-1. (d) The ratio of nuclear Nrf2 to cytosolic Nrf2. Bands were semi-quantitatively analyzed using the ImageJ software and normalized to GAPDH or Histone H3. Data are presented as mean \pm SD (n=3). *p<0.05 vs. vehicle group, **p<0.01 vs. vehicle group. The samples were derived from the same experiment and the gels/blots were processed in parallel.

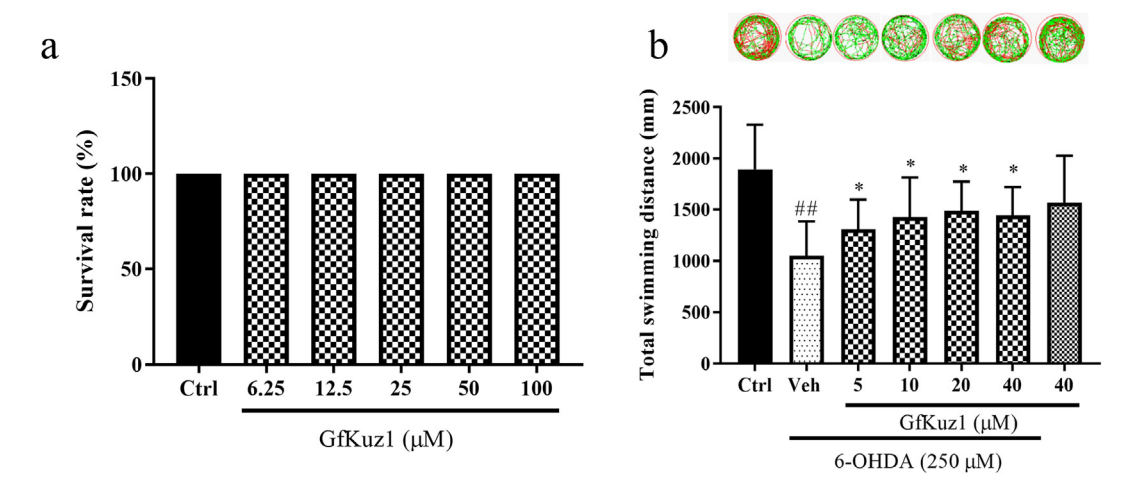


Fig. 9. (a) Survival rates of zebrafish larvae (6 days post-fertilization) exposed to an increasing concentration of GfKuz1 for 24 h. The larvae were transferred into a 96-well plate, one larva per well. (b) The larvae were acclimated for 20 min and the swimming distances were recorded for 10 min. The trajectory of zebrafish swimming in a 96-well plate is depicted in the top of the histogram. Instantaneous velocity is represented by different colors (black, <2 mm/s; green, 2-8 mm/s; red, >8 mm/s). Data are presented as mean \pm SD (n=12). ##p<0.01 vs. control group, *p<0.05 vs. vehicle group.

inhibitor of Kv1.3.

The PC-12 cell line is a pheochromocytoma of the rat adrenal medulla commonly used *in vitro* to examine neurological diseases. The cell viability assay showed that GfKuz1 is non-toxic to PC-12 cells even at concentrations as high as 100 μ M. Furthermore, 5–10 μ M of GfKuz1 had a superior effect in promoting cell viability, which was down-regulated by 6-OHDA compared with other coral peptides. The potassium currents were also investigated, and GfKuz1 at 10 μ M strongly increased the ion intensity (by almost 30%) compared to the control group, indicating that GfKuz1 had a similar inhibitory effect to some potassium blockers (Fig. 6). In summary, the combination of multiple sequence alignment, neighbor-joining phylogenetic tree construction, molecular docking, MD simulation, cell viability test, and potassium ion fluorescence bioassay all suggested that GfKuz1 potentially represents a common potassium channel inhibitor, particularly as an inhibitor of Kv1.3, although further experimentation is required to substantiate this claim.

ROS contain oxygen and readily react with other molecules in cells (Hayyan et al., 2016). The development of neurological damage is related to ROS generation, which may increase the risk of oxidative damage to neurons (Jakkula et al., 2018). One factor that maintains neural homeostasis is a low level of ROS production, which plays an essential role in signal transduction, gene expression, proliferation, and host defense (Dröge, 2002). Exposure to 6-OHDA causes a high level of ROS, leading to oxidative stress and cellular and DNA damage (Bernstein, Garrison, Zambetti and O'Malley, 2011; Schieber and Chandel, 2014). The ROS-sensitive fluorescent probe 2',7'-dichlorofluorescin can be used to detect ROS activity, where increased fluorescence indicates elevated ROS generation (Liu and O'Rourke, 2001). In the present study, the production of ROS was about 4-fold higher after treatment with 6-OHDA compared with the control group, and 2.5-10 µM of GfKuz1 peptide reduced the level of ROS, which indicated that GfKuz1 could inhibit the generation of ROS and thus mitigates 6-OHDA neurotoxicity.

The Nrf2 signaling pathway is considered a novel potential treatment target for neurodegenerative diseases (Lee et al., 2012). Under normal conditions, Keap1 exerts an inhibitory effect on the transcriptional activity of Nrf2 by blocking proteasomal degradation and ubiquitination (Tebay et al., 2015). After being exposed to 6-OHDA, excessive generation of ROS modified cysteine residues in Keap1, and the degradative effect of Nrf2 is thus attenuated (Kensler and Wakabayashi, 2010). The binding site of Nrf2 in the cytoplasm was released from Keap1 and translocated into the nucleus. Small Maf proteins interacted with Nrf2 and generated a homodimer. HO-1 is the inducible isoform of HO and plays a critical function in oxidative cleavage (Araujo et al., 2012). After binding with the ARE-sequence, cytoprotective HO-1 gene expression was induced and oxidative stress was alleviated (Hayes et al., 2010). Like some drugs, 6-OHDA upregulated Keap1, which indicated neurotoxic effects, i.e., increased release rates for Nrf2 and Keap1 (Chen et al., 2021; Gao et al., 2018; Huang et al., 2016). 5-10 µM of GfKuz1 increased the protective effect. Furthermore, 6-OHDA caused the translocation of Nrf2 from the cytoplasm to the nucleus and increased the expression of HO-1. The results indicated that GfKuz1 elevated the nuclear level of Nrf2 and thus up-regulated the gene expression of HO-1. The results also demonstrated that GfKuz1 promoted the translocation of Nrf2 from the cytoplasm to the nucleus and enhanced the expression of HO-1 under oxidative stress (Fig. 8).

This study had some limitations. In general, Kunitz-type peptides contain three disulfide bonds (C1–C6, C2–C4, and C3–C5) that maintain their stability and attenuate degradation by some proteases (Goldberg, 2003). We did not fold the disulfide bonds but employed MD simulation to predict the stability of the peptides. Regarding the molecular docking results, it would be preferable to include the mutations of some residues in GfKuz1 to test the affinity to $K_V1.3$ and perform *in vivo* and *in vitro* studies. Complementary mutagenesis and thermodynamic mutant cycle analysis are good methods for the functional interaction surfaces and energetic interactions between the inhibitor and the channel. These docking configurations need to be experimentally validated in the future

(Ranganathan et al., 1996). Kunitz-bovine pancreatic trypsin inhibitor, a peptide containing a Kunitz-type domain from the bovine pancreas, crosses the blood-brain barrier via low-density lipoprotein receptor-related protein (LRP) (Cankurtaran-Sayar et al., 2009; Kounnas et al., 1995). Furthermore, short peptides provide the basis for the Kunitz-bovine pancreatic trypsin inhibitor sequence, which have been shown to cross the blood-brain barrier with high effectiveness. Potentially, some Kunitz domain-derived peptides could be used in a novel brain delivery system (Demeule et al., 2008). The studied peptides have the same Kunitz domain, including the pattern responsible for penetration through the blood-brain barrier. Furthermore, an enhancement of potassium currents could lead to oxidant-induced apoptosis (McLaughlin et al., 2001). We reported data regarding the investigation of the attenuation of ROS levels and involvement of the Nrf2 pathway in PC-12 cells in response to the GfKuz1 coral peptide.

Zebrafish have been employed in the investigation of various neuropsychiatric and neurodegenerative human diseases, due to the fish having similarities to human brain physiology and anatomy (Fontana et al., 2018). Zebrafish genomes exhibit a 70% homology with those of humans. Intramuscular injections of 6-OHDA in zebrafish resulted in locomotor impairments and reduced dopamine levels, making it a classical model for studying PD (Doyle and Croll, 2022). After administration of 6-OHDA, the swimming distance of zebrafish was reduced compared with control groups. GfKuz1 reversed the abnormal swimming behavior which demonstrated that GfKuz1 exerts neuroprotective effects *in vivo*.

We focused on the antioxidative effect of GfKuz1 while the neuro-inflammatory effect of GfKuz1 has not been investigated. However, dysregulation of NOD-like receptor P3 (NLRP3) inflammasome could be involved in the development of neurodegenerative diseases which activated NLRP3. GfKuz1 could suppress the potassium efflux which indicates that GfKuz1 may inhibit the activation of NLRP3 and thus exert an anti-inflammatory effect (Xu et al., 2020). Further studies are needed to understand the anti-inflammatory effect of GfKuz1 on various PD models.

5. Conclusions

Marine biota, particularly in the phylum Cnidaria, have long been recognized as a rich source of bioactive compounds with promising therapeutic potential. This study employed bioinformatic tools to analyze the transcriptomic data of the octocoral G. fascicularis, leading to the identification of a novel Kunitz peptide for the treatment of Parkinson's disease. The proposed mechanism involves the blockade of $K_V1.3$ channels and the activation of the Nrf2 signaling pathway. These findings not only offer a new strategy for discovering bioactive peptides targeting potassium ion channels but also highlight the potential of this novel peptide as a candidate drug for Parkinson's disease.

CRediT authorship contribution statement

Hanbin Chen: Software, Methodology, Investigation, Data curation, Conceptualization. Hiotong Kam: Methodology, Formal analysis, Data curation, Conceptualization. Shirley Weng In Siu: Methodology, Formal analysis, Data curation. Clarence Tsun Ting Wong: Methodology, Formal analysis, Data curation. Jian-Wen Qiu: Writing – review & editing, Writing – original draft, Supervision, Funding acquisition. Alex Kwok-Kuen Cheung: Writing – review & editing, Writing – original draft. Gandhi Rádis-Baptista: Writing – review & editing, Writing – original draft. Simon Ming-Yuen Lee: Writing – review & editing, Writing – original draft, Visualization, Validation, Supervision, Resources, Project administration, Investigation, Funding acquisition.

Ethical Statement

The study was approved by Animal Research Ethics Committee of the University of Macau, China (ethics number: UMARE-021b-2020). All

methods were carried out in accordance with relevant guidelines and regulations. This study was carried out in compliance with the Animal Research: Reporting of *In Vivo* Experiments (ARRIVE) guidelines.

Funding

This work was supported by the China Postdoctoral Science Foundation under Grant Number 2023M731524, University of Macau and funded by The Science and Technology Development Fund (FDTC) of Macau SAR (File no. 0058/2019/A1 and 0016/2019/AKP), University of Macau (MYRG2019-00105-ICMS) and The Hong Kong Polytechnic University (Project ID. P0006304). The Environmental and Conservation Fund of Hong Kong (grant no. 34/2019), and Key Special Project for Introduced Talents Team of Southern Marine Science and Engineering Guangdong laboratory (Guangzhou) (grant nos. GMl2019ZD0404, SMSEGl20SC02). This work was performed in part at the high performance computing cluster (HPCC) which is supported by the Information and Communication Technology office (ICTO) of the University of Macau.

Declaration of competing Interest

Simon Ming-Yuen Lee is an editorial board member for Water Biology and Security and was not involved in the editorial review or the decision to publish this article.

Appendix A. Supplementary data

Supplementary data to this article can be found online at https://doi.org/10.1016/j.watbs.2025.100358.

References

- Adasme, M.F., Linnemann, K.L., Bolz, S.N., Kaiser, F., Salentin, S., Haupt, V.J., Schroeder, M., 2021. Plip 2021: expanding the scope of the protein-ligand interaction profiler to DNA and RNA. Nucleic Acids Res. 49 (W1), W530–W534. https://doi.org/10.1093/nar/gkab294.
- Araujo, J.A., Zhang, M., Yin, F., 2012. Heme oxygenase-1, oxidation, inflammation, and atherosclerosis. Front. Pharmacol. 3, 119. https://doi.org/10.3389/ fphar.2012.00119.
- Bachmann, M., Li, W., Edwards, M.J., Ahmad, S.A., Patel, S., Szabo, I., Gulbins, E., 2020. Voltage-gated potassium channels as regulators of cell death. Front. Cell Dev. Biol. 8 (1571). https://doi.org/10.3389/fcell.2020.611853.
- Baker, N.A., Sept, D., Joseph, S., Holst, M.J., McCammon, J.A., 2001. Electrostatics of nanosystems: application to microtubules and the ribosome. Proc. Natl. Acad. Sci. USA 98 (18), 10037–10041. https://doi.org/10.1073/pnas.181342398.
- Benkert, P., Biasini, M., Schwede, T., 2010. Toward the estimation of the absolute quality of individual protein structure models. Bioinformatics 27 (3), 343–350. https:// doi.org/10.1093/bioinformatics/btq662.
- Bernstein, A.I., Garrison, S.P., Zambetti, G.P., O'Malley, K.L., 2011. 6-OHDA generated ROS induces DNA damage and p53- and PUMA-dependent cell death. Mol. Neurodegener. 6 (1), 2. https://doi.org/10.1186/1750-1326-6-2.
- Bertoni, M., Kiefer, F., Biasini, M., Bordoli, L., Schwede, T., 2017. Modeling protein quaternary structure of homo- and hetero-oligomers beyond binary interactions by homology. Sci. Rep. 7 (1), 10480. https://doi.org/10.1038/s41598-017-09654-8.
- Bienert, S., Waterhouse, A., de Beer, Tjaart A.P., Tauriello, G., Studer, G., Bordoli, L., Schwede, T., 2016. The SWISS-MODEL Repository—new features and functionality. Nucleic Acids Res. 45 (D1), D313–D319. https://doi.org/10.1093/nar/gkw1132.
- Boldrini-França, J., Pinheiro-Junior, E.L., Peigneur, S., Pucca, M.B., Cerni, F.A., Borges, R.J., Costa, T.R., Carone, S.E.I., Fontes, M.R.d.M., Sampaio, S.V., et al., 2020. Beyond hemostasis: a snake venom serine protease with potassium channel blocking and potential antitumor activities. Sci. Rep. 10 (1), 4476. https://doi.org/10.1038/ s41598-020-61258-x.
- Cadet, J.L., Brannock, C., 1998. Free radicals and the pathobiology of brain dopamine systems. Neurochem. Int. 32 (2), 117–131. https://doi.org/10.1016/s0197-0186(97) 00021.4
- Cankurtaran-Sayar, S., Sayar, K., Ugur, M., 2009. P2X7 receptor activates multiple selective dye-permeation pathways in RAW 264.7 and human embryonic kidney 293 cells. Mol. Pharmacol. 76 (6), 1323–1332. https://doi.org/10.1124/mol.109.059923.
- Chen, J., Chen, Y., Zheng, Y., Zhao, J., Yu, H., Zhu, J., Li, D., 2021. Protective effects and mechanisms of procyanidins on Parkinson's disease in vivo and in vitro. Molecules 26 (18). https://doi.org/10.3390/molecules26185558.
- Chen, X., Guo, C., Kong, J., 2012. Oxidative stress in neurodegenerative diseases. Neural Regen. Res. 7 (5), 376–385. https://doi.org/10.3969/j.issn.1673-5374.2012.05.009.

- Chen, X., Xue, B., Wang, J., Liu, H., Shi, L., Xie, J., 2018. Potassium channels: a potential therapeutic target for Parkinson's disease. Neurosci. Bull. 34 (2), 341–348. https:// doi.org/10.1007/s12264-017-0177-3.
- Cronin, A., Grealy, M., 2017. Neuroprotective and Neuro-restorative effects of Minocycline and Rasagiline in a zebrafish 6-hydroxydopamine model of Parkinson's disease. Neuroscience 367, 34–46. https://doi.org/10.1016/j.neuroscience.2017.10.018.
- D'Ambra, I., Lauritano, C., 2020. A review of toxins from cnidaria. Mar. Drugs 18 (10), 507. https://doi.org/10.3390/md18100507.
- Deffains, M., Bergman, H., 2015. Striatal cholinergic interneurons and cortico-striatal synaptic plasticity in health and disease. Mov. Dis.: off. j. Mov. Disord. Society 30 (8), 1014–1025. https://doi.org/10.1002/mds.26300.
- DeMaagd, G., Philip, A., 2015. Parkinson's disease and its management: part 1: Disease entity, risk factors, pathophysiology, clinical presentation, and diagnosis, 40 (2015/ 08/04 ed.): Pt.
- Demeule, M., Currie, J.C., Bertrand, Y., Ché, C., Nguyen, T., Régina, A., Gabathuler, R., Castaigne, J.P., Béliveau, R., 2008. Involvement of the low-density lipoprotein receptor-related protein in the transcytosis of the brain delivery vector angiopep-2. J. Neurochem. 106 (4), 1534–1544. https://doi.org/10.1111/j.1471-4159.2008.05492.x.
- Doyle, J.M., Croll, R.P., 2022. A critical review of zebrafish models of Parkinson's disease. Front. Pharmacol. 13, 835827. https://doi.org/10.3389/fphar.2022.835827.
- Dröge, W., 2002. Free radicals in the physiological control of cell function. Physiol. Rev. 82 (1), 47–95. https://doi.org/10.1152/physrev.00018.2001.
- Federico, A., Cardaioli, E., Da Pozzo, P., Formichi, P., Gallus, G.N., Radi, E., 2012. Mitochondria, oxidative stress and neurodegeneration. J. Neurol. Sci. 322 (1–2), 254–262. https://doi.org/10.1016/j.jns.2012.05.030.
- Felsenstein, J., 1985. Confidence limits on phylogenies: an approach using the bootstrap. Evolution 39 (4), 783–791. https://doi.org/10.1111/j.1558-5646.1985.tb00420.x.
- Fischer, R., Maier, O., 2015. Interrelation of oxidative stress and inflammation in neurodegenerative disease: role of TNF. Oxid. Med. Cell. Longev. 2015, 610813. https://doi.org/10.1155/2015/610813.
- Fontana, B.D., Mezzomo, N.J., Kalueff, A.V., Rosemberg, D.B., 2018. The developing utility of zebrafish models of neurological and neuropsychiatric disorders: A critical review. Exp. Neurol. 299 (Pt A), 157–171. https://doi.org/10.1016/ j.expneurol.2017.10.004.
- Gao, J., Liu, S., Xu, F., Liu, Y., Lv, C., Deng, Y., Shi, J., Gong, Q., 2018. Trilobatin protects against oxidative injury in neuronal PC12 cells through regulating mitochondrial ROS homeostasis mediated by AMPK/Nrf2/Sir13 signaling pathway. Front. Mol. Neurosci. 11 (267). https://doi.org/10.3389/fnmol.2018.00267.
- Goldberg, A.L., 2003. Protein degradation and protection against misfolded or damaged proteins. Nature 426 (6968), 895–899. https://doi.org/10.1038/nature02263.
- Gouda, N.A., Cho, J., 2022. Omarigliptin mitigates 6-hydroxydopamine- or rotenone-induced oxidative toxicity in PC12 cells by antioxidant, anti-inflammatory, and anti-apoptotic actions. Antioxidants 11 (10). https://doi.org/10.3390/antiox11101940.
- Guex, N., Peitsch, M.C., Schwede, T., 2009. Automated comparative protein structure modeling with SWISS-MODEL and Swiss-PdbViewer: a historical perspective. Electrophoresis 30 (S1), S162–S173. https://doi.org/10.1002/elps.200900140.
- Harish, B.S., Uppuluri, K.B., 2018. Microbial serine protease inhibitors and their therapeutic applications. Int. J. Biol. Macromol. 107 (Pt B), 1373–1387. https://doi.org/10.1016/j.ijbiomac.2017.09.115.
- Hayes, J.D., McMahon, M., Chowdhry, S., Dinkova-Kostova, A.T., 2010. Cancer chemoprevention mechanisms mediated through the Keap1-Nrf2 pathway. Antioxidants Redox Signal. 13 (11), 1713–1748. https://doi.org/10.1089/ ars 2010 3221
- Hayyan, M., Hashim, M.A., AlNashef, I.M., 2016. Superoxide ion: generation and Chemical Implications. Chemical reviews 116 (5), 3029–3085. https://doi.org/ 10.1021/acs.chemics.5b00407
- Hemmati-Dinarvand, M., Saedi, S., Valilo, M., Kalantary-Charvadeh, A., Alizadeh Sani, M., Kargar, R., Safari, H., Samadi, N., 2019. Oxidative stress and Parkinson's disease: conflict of oxidant-antioxidant systems. Neurosci. Lett. 709, 134296. https://doi.org/10.1016/j.neulet.2019.134296.
- Hemmati-Dinarvand, M., Taher-Aghdam, A.A., Mota, A., Zununi Vahed, S., Samadi, N., 2017. Dysregulation of serum NADPH oxidase1 and ferritin levels provides insights into diagnosis of Parkinson's disease. Clin. Biochem. 50 (18), 1087–1092. https:// doi.org/10.1016/j.clinbiochem.2017.09.014.
- Huang, J.Y., Yuan, Y.H., Yan, J.Q., Wang, Y.N., Chu, S.F., Zhu, C.G., Guo, Q.L., Shi, J.G., Chen, N.H., 2016. 20C, a bibenzyl compound isolated from Gastrodia elata, protects PC12 cells against rotenone-induced apoptosis via activation of the Nrf2/ARE/HO-1 signaling pathway. Acta Pharmacol. Sin. 37 (6), 731–740. https://doi.org/10.1038/ aps.2015.154.
- Itoh, K., Wakabayashi, N., Katoh, Y., Ishii, T., Igarashi, K., Engel, J.D., Yamamoto, M., 1999. Keap1 represses nuclear activation of antioxidant responsive elements by Nrf2 through binding to the amino-terminal Neh2 domain. Gene Dev. 13 (1), 76–86. https://doi.org/10.1101/gad.13.1.76.
- Jakkula, P., Reinikainen, M., Hästbacka, J., Loisa, P., Tiainen, M., Pettilä, V., Toppila, J., Lähde, M., Bäcklund, M., Okkonen, M., et al., 2018. Targeting two different levels of both arterial carbon dioxide and arterial oxygen after cardiac arrest and resuscitation: a randomised pilot trial. Intensive Care Med. 44 (12), 2112–2121. https://doi.org/ 10.1007/s00134-018-5453-9.
- Jo, S., Kim, T., Im, W., 2007. Automated builder and database of protein/membrane complexes for molecular dynamics simulations. PLoS One 2 (9), e880. https:// doi.org/10.1371/journal.pone.0000880 e880.
- Jo, S., Kim, T., Iyer, V.G., Im, W., 2008. CHARMM-GUI: a web-based graphical user interface for CHARMM. J. Comput. Chem. 29 (11), 1859–1865. https://doi.org/ 10.1002/jcc.20945.

- Jo, S., Lim, J.B., Klauda, J.B., Im, W., 2009. CHARMM-GUI Membrane Builder for mixed bilayers and its application to yeast membranes. Biophys. J. 97 (1), 50–58. https:// doi.org/10.1016/j.bpj.2009.04.013.
- Kensler, T.W., Wakabayashi, N., 2010. Nrf2: friend or foe for chemoprevention? Carcinogenesis 31 (1), 90–99. https://doi.org/10.1093/carcin/bgp231.
- Kim, G.H., Kim, J.E., Rhie, S.J., Yoon, S., 2015. The role of oxidative stress in neurodegenerative diseases. Exp. Neurobiol. 24 (4), 325–340. https://doi.org/ 10.5607/en.2015.24.4.325.
- Kim, S., Ko, D., Lee, Y., Jang, S., Lee, Y., Lee, I.Y., Kim, S., 2019. Anti-cancer activity of the novel 2-hydroxydiarylamide derivatives IMD-0354 and KRT1853 through suppression of cancer cell invasion, proliferation, and survival mediated by TMPRSS4. Sci. Rep. 9 (1), 10003. https://doi.org/10.1038/s41598-019-46447-7.
- Klompen, A.M.L., Macrander, J., Reitzel, A.M., Stampar, S.N., 2020. Transcriptomic analysis of four cerianthid (Cnidaria, Ceriantharia) venoms. Mar. Drugs 18 (8), 413. https://doi.org/10.3390/md18080413.
- Kounnas, M.Z., Moir, R.D., Rebeck, G.W., Bush, A.I., Argraves, W.S., Tanzi, R.E., Hyman, B.T., Strickland, D.K., 1995. LDL receptor-related protein, a multifunctional ApoE receptor, binds secreted beta-amyloid precursor protein and mediates its degradation. Cell 82 (2), 331–340. https://doi.org/10.1016/0092-8674(95)90320-8.
- Kumar, S., Stecher, G., Li, M., Knyaz, C., Tamura, K., 2018. MEGA X: Molecular evolutionary genetics analysis across computing platforms. Mol. Biol. Evol. 35 (6), 1547–1549. https://doi.org/10.1093/molbev/msy096.
- Lawson, K., McKay, N.G., 2006. Modulation of potassium channels as a therapeutic approach. Curr. Pharmaceut. Des. 12 (4), 459–470. https://doi.org/10.2174/ 138161206775474477.
- Lee, D.H., Gold, R., Linker, R.A., 2012. Mechanisms of oxidative damage in multiple sclerosis and neurodegenerative diseases: therapeutic modulation via fumaric acid esters. Int. J. Mol. Sci. 13 (9), 11783–11803. https://doi.org/10.3390/ iims130911783.
- Lee, J., Cheng, X., Swails, J.M., Yeom, M.S., Eastman, P.K., Lemkul, J.A., Wei, S., Buckner, J., Jeong, J.C., Qi, Y., et al., 2016. CHARMM-GUI input generator for NAMD, GROMACS, AMBER, OpenMM, and CHARMM/OpenMM simulations using the CHARMM36 additive force field. J. Chem. Theor. Comput. 12 (1), 405–413. https://doi.org/10.1021/acs.jctc.5b00935.
- Liao, Q., Gong, G., Poon, T.C.W., Ang, I.L., Lei, K.M.K., Siu, S.W.I., Wong, C.T.T., Rádis-Baptista, G., Lee, S.M., 2019. Combined transcriptomic and proteomic analysis reveals a diversity of venom-related and toxin-like peptides expressed in the mat anemone Zoanthus natalensis (Cnidaria, Hexacorallia). Arch. Toxicol. 93 (6), 1745–1767. https://doi.org/10.1007/s00204-019-02456-z.
- Liao, Q., Li, S., Siu, S.W.I., Yang, B., Huang, C., Chan, J.Y., Morlighem, J.R.L., Wong, C.T.T., Rádis-Baptista, G., Lee, S.M., 2018. Novel Kunitz-like peptides discovered in the Zoanthid Palythoa caribaeorum through transcriptome sequencing. J. Proteome Res. 17 (2), 891–902. https://doi.org/10.1021/acs.jproteome.7b00686.
- Lin, C., Lin, K., Luong, Y.P., Rao, B.G., Wei, Y.Y., Brennan, D.L., Fulghum, J.R., Hsiao, H.M., Ma, S., Maxwell, J.P., et al., 2004. In vitro resistance studies of hepatitis C virus serine protease inhibitors, VX-950 and BILN 2061: structural analysis indicates different resistance mechanisms. J. Biol. Chem. 279 (17), 17508–17514. https://doi.org/10.1074/jbc.M313020200.
- Liu, S., Zhao, Y., Dong, H., Xiao, L., Zhang, Y., Yang, Y., Ong, S.T., Chandy, K.G., Zhang, L., Tian, C., 2021. Structures of wild-type and H451N mutant human lymphocyte potassium channel K(V)1.3. Cell discovery 7 (1), 39. https://doi.org/ 10.1038/s41421-021-00269-y.
- Liu, Y., O'Rourke, B., 2001. Opening of mitochondrial K(ATP) channels triggers cardioprotection. Are reactive oxygen species involved? Circ. Res. 88 (8), 750–752. https://doi.org/10.1161/hh0801.090537.
- Ma, Q., 2013. Role of nrf2 in oxidative stress and toxicity. Annu. Rev. Pharmacol. Toxicol. 53, 401-426. https://doi.org/10.1146/annurev-pharmtox-011112-140320.
- McLaughlin, B., Pal, S., Tran, M.P., Parsons, A.A., Barone, F.C., Erhardt, J.A., Aizenman, E., 2001. p38 activation is required upstream of potassium current enhancement and caspase cleavage in thiol oxidant-induced neuronal apoptosis. J. Neurosci.: the official journal of the Society for Neuroscience 21 (10), 3303–3311. https://doi.org/10.1523/jneurosci.21-10-03303.2001.
- Mirza, M.U., Mirza, A.H., Ghori, N.U., Ferdous, S., 2015. Glycyrrhetinic acid and E.resveratroloside act as potential plant derived compounds against dopamine receptor D3 for Parkinson's disease: a pharmacoinformatics study. Drug design, development and therapy 9, 187–198. https://doi.org/10.2147/dddt.S72794.
- Mistry, J., Chuguransky, S., Williams, L., Qureshi, M., Salazar, G.A., Sonnhammer, E.L.L., Tosatto, S.C.E., Paladin, L., Raj, S., Richardson, L.J., et al., 2021. Pfam: The protein families database in 2021. Nucleic Acids Res. 49 (D1), D412–D419. https://doi.org/ 10.1093/nar/gkaa913.
- Pierce, B.G., Wiehe, K., Hwang, H., Kim, B.H., Vreven, T., Weng, Z., 2014. ZDOCK server: interactive docking prediction of protein-protein complexes and symmetric

- multimers. Bioinformatics 30 (12), 1771–1773. https://doi.org/10.1093/bioinformatics/btu097.
- Peterson, L.J., Flood, P.M., 2012. Oxidative stress and microglial cells in Parkinson's disease. Mediat. Inflamm. 2012, 401264. https://doi.org/10.1155/2012/401264
- Ptak, R., 1990. Notes on the Word Shanhu and Chinese Coral Imports from Maritime Asia c.1250-1600, 39. Archipel: studes interdisciplinaires sur le monde insulindien, pp. 65–80. https://doi.org/10.3406/arch.1990.2621.
- Qi, Y., Liu, H., Daniels, M.P., Zhang, G., Xu, H., 2016. Loss of Drosophila i-AAA protease, dYME1L, causes abnormal mitochondria and apoptotic degeneration. Cell Death Differ. 23 (2), 291–302. https://doi.org/10.1038/cdd.2015.94.
- Ranganathan, R., Lewis, J.H., MacKinnon, R., 1996. Spatial localization of the K+ channel selectivity filter by mutant cycle-based structure analysis. Neuron 16 (1), 131–139. https://doi.org/10.1016/s0896-6273(00)80030-6.
- Ren, G., Zhang, X., Xiao, Y., Zhang, W., Wang, Y., Ma, W., Wang, X., Song, P., Lai, L., Chen, H., et al., 2019. ABRO1 promotes NLRP3 inflammasome activation through regulation of NLRP3 deubiquitination. The EMBO journal 38 (6). https://doi.org/ 10.15252/embi.2018100376.
- Rocha, J., Peixe, L., Gomes, N.C., Calado, R., 2011. Cnidarians as a source of new marine bioactive compounds-an overview of the last decade and future steps for bioprospecting. Mar. Drugs 9 (10), 1860–1886. https://doi.org/10.3390/ md9101860.
- Saitou, N., Nei, M., 1987. The neighbor-joining method: a new method for reconstructing phylogenetic trees. Mol. Biol. Evol. 4 (4), 406–425. https://doi.org/10.1093/ oxfordjournals.molbev.a040454.
- Sanders, L.H., Timothy Greenamyre, J., 2013. Oxidative damage to macromolecules in human Parkinson disease and the rotenone model. Free Radical Biol. Med. 62, 111–120. https://doi.org/10.1016/j.freeradbiomed.2013.01.003.
- Schieber, M., Chandel, N.S., 2014. ROS function in redox signaling and oxidative stress. Curr. Biol.: CB 24 (10), R453–R462. https://doi.org/10.1016/j.cub.2014.03.034.
- Sekar, P., Huang, D.Y., Chang, S.F., Lin, W.W., 2018. Coordinate effects of P2X7 and extracellular acidification in microglial cells. Oncotarget 9 (16), 12718–12731. https://doi.org/10.18632/oncotarget.24331.
- Soualmia, F., El Amri, C., 2018. Serine protease inhibitors to treat inflammation: a patent review (2011-2016). Expert Opin. Ther. Pat. 28 (2), 93–110. https://doi.org/10.1080/13543776.2018.1406478.
- Taguchi, K., Motohashi, H., Yamamoto, M., 2011. Molecular mechanisms of the Keapl—Nrf2 pathway in stress response and cancer evolution. Genes cell.: devoted to Mol. Cell. Mech. 16 (2), 123–140. https://doi.org/10.1111/j.1365-2443.2010.01473.x.
- Taherian, R., Mehran Arab, A., 2015. 4-aminopyridine decreases MPTP-induced behavioral disturbances in animal model of Parkinson's disease. International Clinical Neuroscience Journal 2 (4), 142–146. https://doi.org/10.22037/icnj.v2i4.11791.
- Tebay, L.E., Robertson, H., Durant, S.T., Vitale, S.R., Penning, T.M., Dinkova-Kostova, A.T., Hayes, J.D., 2015. Mechanisms of activation of the transcription factor Nrf2 by redox stressors, nutrient cues, and energy status and the pathways through which it attenuates degenerative disease. Free radical biology & medicine 88 (Pt B), 108–146. https://doi.org/10.1016/j.freeradbiomed.2015.06.021.
- Tubert, C., Taravini, I.R.E., Flores-Barrera, E., Sánchez, G.M., Prost, M.A., Avale, M.E., Tseng, K.Y., Rela, L., Murer, M.G., 2016. Decrease of a current mediated by Kv1.3 channels causes Striatal Cholinergic Interneuron hyperexcitability in experimental parkinsonism. Cell Rep. 16 (10), 2749–2762. https://doi.org/10.1016/j.celrep.2016.08.016.
- Waterhouse, A., Bertoni, M., Bienert, S., Studer, G., Tauriello, G., Gumienny, R., Heer, F.T., de Beer, T.A.P., Rempfer, C., Bordoli, L., et al., 2018. SWISS-MODEL: homology modelling of protein structures and complexes. Nucleic Acids Res. 46 (W1), W296–W303. https://doi.org/10.1093/nar/gky427.
- Westerfield, M.A., 2000. Guide for the Laboratory Use of Zebrafish (Danio rerio) Eugene, fourth ed. OR. University of Oregon Press, USA. Eugene.
- Williamson, T.P., Johnson, D.A., Johnson, J.A., 2012. Activation of the Nrf2-ARE pathway by siRNA knockdown of Keap1 reduces oxidative stress and provides partial protection from MPTP-mediated neurotoxicity. Neurotoxicology 33 (3), 272–279. https://doi.org/10.1016/j.neuro.2012.01.015.
- Wulff, H., Castle, N.A., Pardo, L.A., 2009. Voltage-gated potassium channels as therapeutic targets. Nat. Rev. Drug Discov. 8 (12), 982–1001. https://doi.org/ 10.1038/nrd2983.
- Xu, Z., Chen, Z.M., Wu, X., Zhang, L., Cao, Y., Zhou, P., 2020. Distinct molecular mechanisms underlying potassium efflux for NLRP3 inflammasome activation. Front. Immunol. 11, 609441. https://doi.org/10.3389/fimmu.2020.609441.
- Zhang, Y., Chen, Q., Xie, J.Y., Yeung, Y.H., Xiao, B., Liao, B., Xu, J., Qiu, J.W., 2019. Development of a transcriptomic database for 14 species of scleractinian corals. BMC Genom. 20 (1), 387. https://doi.org/10.1186/s12864-019-5744-8.